The guanine nucleotide exchange factor GBF1 participates in rotavirus replication

Martínez, José L ; Arnoldi, Francesca ; Schraner, Elisabeth M ; Eichwald, Catherine ; Silva-Ayala, Daniela ; Lee, Eunjoo ; Sztul, Elizabeth ; Burrone, Óscar R ; López, Susana ; Arias, Carlos F

Abstract: Cellular and viral factors participate in the replication cycle of rotavirus. We report that the guanine nucleotide exchange factor GBF1, which activates the small GTPase Arf1 to induce COPI transport processes, is required for rotavirus replication since knocking down GBF1 expression by RNA interference, or inhibiting its activity by treatment with Brefeldin A (BFA) or Golgicide A (GCA) significantly reduce the yield of infectious viral progeny. This reduction in virus yield was related to a block in virus assembly since in the presence of either BFA or GCA the assembly of infectious mature triple-layered virions was significantly prevented and only doubled layered-particles were detected. We report that the catalytic activity of GBF1, but not the activation of Arf1, is essential for the assembly of the outer capsid of rotavirus. We show that both BFA and GCA, as well as interfering with the synthesis of GBF1, alter the electrophoretic mobility of glycoproteins VP7 and NSP4 and block the trimerization of the virus surface VP7, a step required for its incorporation into virus particles. Although a post-translational modification of VP7 (other than glycosylation) could be related to the lack of trimerization, we found that NSP4 might also be involved in this process, since knocking-down its expression reduces VP7 trimerizarion. In support, recombinant VP7 protein overexpressed in transfected cells formed trimers only when co-transfected with NSP4. <jats:bold>IMPORTANCE</jats:bold> Rotavirus, a member of the family Reoviridae, is the major cause of severe diarrhea in children and young animals worldwide. Despite the significant advances in the characterization of the biology of this virus, the mechanisms involved in morphogenesis of the virus particle are still poorly understood. In this work, we show that the guanine nucleotide exchange factor GBF1, relevant for the COPI/Arf1-mediated cellular vesicular transport, participates in the replication cycle of the virus, influencing the correct processing of viral glycoproteins VP7 and NSP4, and the assembly of the virus surface proteins VP7 and VP4.

DOI: https://doi.org/10.1128/jvi.01062-19

The guanine nucleotide exchange factor GBF1 participates in rotavirus replication

José L. Martínez[a], Francesca Arnoldi[b,c], Elisabeth M. Schraner[d], Catherine Eichwald[d], Daniela Silva-Ayala[a*], Eunjoo Lee[e], Elizabeth Sztul[e], Óscar R. Burrone[b], Susana López[a], and Carlos F. Arias[a#].

[a]Instituto de Biotecnología, Universidad Nacional Autónoma de México, Cuernavaca, Morelos, México.

[b]International Centre for Genetic Engineering and Biotechnology, Trieste, Italy

[c]Department of Medicine, Surgery and Health Sciences, University of Trieste, Trieste, Italy

[d]Institute of Virology, University of Zurich, Zurich, Switzerland

[e] Department of Cell Biology, University of Alabama at Birmingham, Birmingham, Alabama, USA.

[*]Present address: Daniela Silva-Ayala, Center for Virology and Vaccine Research, Harvard Medical School, Boston, Massachusetts, USA

Running head: Assembly of rotavirus surface proteins

#Address correspondence to: Carlos F. Arias, arias@ibt.unam.mx.

Keywords: rotavirus, morphogenesis, GBF1 nucleotide exchange factor

Word Counts: Abstract: 223; Main text: 8,603

ABSTRACT

Cellular and viral factors participate in the replication cycle of rotavirus. We report that the guanine nucleotide exchange factor GBF1, which activates the small GTPase Arf1 to induce COPI transport processes, is required for rotavirus replication since knocking down GBF1 expression by RNA interference, or inhibiting its activity by treatment with Brefeldin A (BFA) or Golgicide A (GCA) significantly reduce the yield of infectious viral progeny. This reduction in virus yield was related to a block in virus assembly since in the presence of either BFA or GCA the assembly of infectious mature triple-layered virions was significantly prevented and only doubled layered-particles were detected. We report that the catalytic activity of GBF1, but not the activation of Arf1, is essential for the assembly of the outer capsid of rotavirus. We show that both BFA and GCA, as well as interfering with the synthesis of GBF1, alter the electrophoretic mobility of glycoproteins VP7 and NSP4 and block the trimerization of the virus surface VP7, a step required for its incorporation into virus particles. Although a post-translational modification of VP7 (other than glycosylation) could be related to the lack of trimerization, we found that NSP4 might also be involved in this process, since knocking-down its expression reduces VP7 trimerizarion. In support, recombinant VP7 protein overexpressed in transfected cells formed trimers only when co-transfected with NSP4.

40 **IMPORTANCE**

41 Rotavirus, a member of the family Reoviridae, is the major cause of severe diarrhea in
42 children and young animals worldwide. Despite the significant advances in the
43 characterization of the biology of this virus, the mechanisms involved in morphogenesis of
44 the virus particle are still poorly understood. In this work, we show that the guanine
45 nucleotide exchange factor GBF1, relevant for the COPI/Arf1-mediated cellular vesicular
46 transport, participates in the replication cycle of the virus, influencing the correct
47 processing of viral glycoproteins VP7 and NSP4, and the assembly of the virus surface
48 proteins VP7 and VP4.

49

50

51

52

53

54

55

56

57

58

INTRODUCTION

Rotaviruses, members of the family *Reoviridae*, are non-enveloped particles formed by three concentric layers of proteins that surround the eleven genome segments of double-stranded RNA (dsRNA). The innermost layer is composed of the core-shell proteinVP2 that encloses the replication intermediates, composed of the RNA dependent RNA polymerase VP1, and the guanylyl-methyl transferase, VP3. The intermediate layer is formed by VP6 that surrounds the VP2 layer to form double-layered particles (DLPs). Finally, the addition of the glycoprotein VP7 and the spike protein VP4 onto the DLPs forms the infectious triple-layered particles (TLPs) (1, 2).

The replication of rotavirus occurs in cytoplasmic non-membranous electron-dense inclusions termed viroplasms composed of NSP2, NSP5, VP1, VP2, VP6 and host components (1, 3). The replication and packaging of the viral genome into newly synthesized DLPs take place in these inclusions (4), which then bud into the lumen of the endoplasmic reticulum (ER) through membrane sites modified by the presence of NSP4 (5, 6). NSP4 is a transmembrane ER glycoprotein with two N-linked high mannose glycosylated chains (7) that play a crucial role in the last steps of rotavirus assembly. It has been shown that the cytoplasm oriented-terminus of NSP4 associates with VP4 (8), and binds the VP6 on DLPs acting as a receptor for these particles to mediate their budding into the ER (9, 10). Moreover, NSP4 has been shown to also interact with VP7 through its N-terminus oriented to the ER lumen (11, 12). It has been proposed that these interactions drive the incorporation of the outer layer proteins into the transitory lipid envelope that DLPs acquire during ER membrane budding; this envelope is removed in the lumen of the ER by an unknown process in which NSP4 is eliminated while VP4 and VP7 are assembled

to produce the final infectious TLPs (13, 14). Although the precise mechanism of the final steps of rotavirus assembly is not well understood, it has been found that VP7 structure forms trimers on the surface of the virion in a calcium-dependent process (15–18).

Due to the high complexity of rotavirus replication, many of the cellular factors and molecular mechanisms involved in this process are poorly characterized. However, it has been recently reported that the coatomer protein I (COPI)/Arf1 machinery is essential for virus replication since knocking-down by RNA interference (RNAi) the expression of some of the proteins that integrate such machinery reduces virus replication (19, 20). Also, brefeldin A (BFA), an inhibitor of the COPI/Arf1-mediated vesicular transport, significantly impairs the rotavirus progeny yield (21). COPI is a protein complex formed by seven subunits (α, β, β′, δ, ε, γ and ζ-COP) that mediates the retrograde transport of vesicles from the Golgi apparatus to the ER (22–24). Besides its canonical functions in the secretory pathway, the COPI/Arf1 machinery also may participate in the maturation of early endosomes and in recycling proteins to the plasma membrane (25, 26), as well as in the maturation of phagosomes (27, 28) and peroxisomes (29). Furthermore, multiple reports suggest that the COPI/Arf1 machinery is also involved in transport events involved in the maturation and function of lipid droplets (LDs) (30–32).

In the initial step of the COPI transport, the small GTPase Arf1 (ADP-ribosylation factor 1) is activated with a GTP molecule in a process catalyzed by the guanine nucleotide exchange factor GBF1 (Golgi-specific BFA resistance factor 1) located at the cis-Golgi membrane and the intermediate ER-Golgi compartment (ERGIC) (33). The activated Arf1-GTP associates with the Golgi membrane and promotes the recruitment of the preformed COPI complex as well as of the Arf1-GTPase-activating protein (Arf1GAP). The formation

105 of Arf1-COPI-Arf1GAP complex stimulates the binding and concentration of different
106 cargoes located in the membrane, association that induces the bending of the membrane
107 into a vesicle. Once completed, the vesicle buds from the membrane covered by the COPI
108 complex proteins. Finally, the coat proteins are disassembled when the GTPase activity of
109 Arf1 is enhanced by Arf1GAP, leading to the hydrolysis of the GTP bound to Arf1. This
110 hydrolysis leads to the release from the membrane of Arf1, COPI, and Arf1GAP (34, 35).

111 GBF1 belongs to a subfamily of large guanine nucleotide exchange factors (GEFs) that also
112 includes the mammalian BIG1, and BIG2 located at the trans-Golgi network (TGN) (36).
113 These three GEFs activate Arf1, however GBF1 may also use Arf4 and Arf5 as substrates
114 (37–39), while BIG1 and BIG2 can catalyze the activation of Arf3, Arf5 and Arf6 (40–42).
115 Arf activation is catalyzed by the Sec7 domain, shared by all GEFs. In addition, GBF1
116 contains five non-catalytic domains: the N-terminal dimerization and cyclophilin binding
117 (DCB), the homology upstream of Sec7 (HUS), and three C-terminal homology
118 downstream of Sec7 (HDS1-3) domains (33, 36). The functions of these non-catalytic
119 domains are not well understood, but the N-terminal DCB and HUS domains have been
120 implicated in inter- and intra-molecular interactions important for GBF1 dimerization and
121 its association to membranes (43, 44), while the HDS1-3 domains have been suggested to
122 facilitate GBF1 association with membranes(45–48).

123 In this study, we evaluated the role of the GBF1/COPI/Arf1 machinery in rotavirus
124 replication. We showed that the catalytic activity of GBF1 is critical for virus replication by
125 using two different pharmacological inhibitors, BFA and Golgicide A (GCA), and
126 knocking down GBF1 expression by RNAi. We found that interfering with GBF1 activity
127 significantly impaired the yield of viral progeny through a block in the assembly of the

virus surface proteins, VP7 and VP4, which prevents the production of mature and infectious TLPs. We also showed that this restriction in the assembly of TLPs is the result of a damage in VP7 trimerization required for its assembly into DLPs. We provide evidence suggesting that the altered post-translational modification of either VP7 or NSP4 in GBF1-inactivated cells is responsible for the defective formation of VP7 trimers. Altogether, our findings suggest that GBF1 activity is essential for the rotavirus outer capsid assembly by allowing the correct processing of VP7 and/or NSP4, possibly through a mechanism independent of Arf1.

RESULTS

Inhibition of GBF1 hinders rotavirus replication. Earlier reports have indicated that the COPI/Arf1 machinery is important for rotavirus replication (19, 20) and we characterized the effects of the pharmacological inhibitors BFA and GCA, which block the GBF1-mediated activation of Arf1 required for COPI transport (34, 35, 49, 50) on the replication of rotaviruses. In these assays, MA104 cells were pretreated for 30 min with different concentrations of BFA or GCA before virus infection. The simian rhesus rotavirus (RRV) was then added to cells in the presence of the inhibitors for 1 h at 37°C. Then, the virus inoculum was removed, and fresh media containing the inhibitors were added; 12 h post infection (hpi), the total virus (from cells and media) was recovered, and the viral yield was determined. We found that treatment with BFA (at a concentration of 0.5 μg/ml or higher) reduced by more than 100-fold the viral yield (Fig 1A); this observation is in agreement with a previous report (21).

149 Similarly, treatment with GCA diminished viral progeny about 50-fold (Fig 1B). Cell
150 treatment with the inhibitors did not alter cell viability at any of the concentrations tested,
151 as determined by an LDH assay (data not shown). Moreover, the reduction of viral yield
152 was independent of the rotavirus strain tested, since BFA also significantly inhibited the
153 replication of SA11 (simian origin), UK (bovine origin), 69M (human origin), and YM
154 (porcine origin) (Fig 1C). However, the extent of inhibition differed among the strains;
155 while the replication of SA11 was reduced to a level similar to RRV (about 100-fold), that
156 of rotavirus strains UK, 69M, and YM was reduced by about 10-fold.

157 To determine whether GBF1 was directly involved in virus replication, we transfected
158 MA104 cells with an siRNA to GBF1, which very efficiently knocked-down the synthesis
159 of this protein (Fig. 1D, left), and 72 h post-transfection (hpt), cells were infected with
160 RRV. After 12 hpi the total virus was harvested, and the viral yield was determined.
161 Silencing the expression of GBF1 reduced the yield of viral progeny by about 70% as
162 compared to that produced in cells transfected with control, irrelevant siRNA (Fig 1D,
163 right). These results, together with the fact that GCA decreases RRV replication to a level
164 similar to that observed with BFA, strongly suggest that GBF1 activity might be involved
165 in the replication cycle of rotaviruses.

166 **BFA and GCA inhibit a post-entry stage of the virus replication cycle.** To evaluate the
167 step of the virus lifecycle affected by BFA and GCA, the drugs were added at different
168 times post-infection to cells infected with RRV, as indicated in Fig. 2A, and at 12 hpi the
169 total virus was recovered, and the viral yield was determined. The addition of the drugs at 0
170 and 2 hpi decreased the viral yield by more than 90%; the inhibitory effect was less evident
171 at subsequent times post-infection. When added at 4 hpi, the drugs reduced only around

60% of the viral progeny production, and at later times they showed no significant inhibitory activity (Fig 2A). The fact that the drugs showed a similar inhibitory effect when pre-incubated with cells or when added 2 hpi suggests that the inhibitors are most likely affecting the replication of RRV at a post-entry step. These findings are in agreement with the previous observation that the effect of silencing the expression of β-COP on virus replication was not relieved by transfection of RRV double-layered particles into the siRNA-treated cells (19). Of interest, the fact that the effect of the drugs seems to decline when added at 4 hpi, time at which the assembly of virus particles has already started (Fig. 2B), suggests that the inhibitors could interfere with the virus assembly process. The similar effect observed for GCA and BFA supports the initial observation that the relevant target for the drugs is GBF1.

BFA and GCA block the production of TLPs. To confirm that the decrease in viral yield was related to a defect in virus assembly, MA104 cells were infected with RRV in the presence of the drugs and the assembly of viral particles was analyzed by CsCl density gradients. In control conditions, two opalescent bands were observed in the gradients (Figs. 3A and 3C), which were shown to correspond to TLPs and DLPs by PAGE analysis (Figs. 3B and 3D). In contrast, in cells treated with BFA or GCA, a single major band that migrated at a density similar to that of DLPs was detected, and by PAGE was shown to contain particles formed exclusively by proteins VP1, VP2 and VP6 (Fig. 3B). These results indicate that the inhibitors block the assembly of the outermost protein layer, formed by VP4 and VP7, onto the correctly assembled DLPs.

These results were confirmed by negative-staining electron microscopy analysis of drug-treated infected cells. For this, MA104 cells were infected with RRV in the presence of the

drugs, and 6 hpi cells were fixed and processed for electron microscopy. In control, untreated cells, typical electro-dense viroplasm structures were observed near the ER membrane. Furthermore, viral particles, presumably DLPs, appear to be budding into the lumen of the ER leading to the formation of membrane-enveloped particles. Many of the viral particles within the ER seem to have lost their lipid envelope and look like mature TLPs (Fig 4A). We found that neither BFA nor GCA prevented the budding of DLPs into the ER to form membrane-enveloped particles; however, the assembly pathway seems to be arrested at this point since the intermediate enveloped particles accumulated within the ER and they did not seem to mature to TLPs (Fig. 4B and 4C). It should be noted that the intermediate membrane-enveloped particles are not detected in the CsCl gradients since they most probably lose their membrane upon with trichloromonofluoromethane extraction, and are rather detected as DLPs.

The electrophoretic mobility of VP7 and NSP4 is altered during the inhibition of GBF1 activity. Since it has been reported that BFA alters the electrophoretic mobility of VP7 and NSP4 (21), we decided to investigate if the effect of GCA in virus assembly was related to a modification of these viral proteins. MA104 cells were infected with RRV in the presence of the inhibitors as described above, and at 7.5 hpi, the cellular proteins were pulse-labeled with ^{35}S-Met for 30 min and chased for 2 h. As seen in Fig. 5A, the inhibitors did not affect the synthesis of either cellular or viral proteins. However, the viral glycoproteins VP7 and NSP4 had modified electrophoretic mobility in the presence of the drugs. In treated cells, VP7 migrated slower than in control cells, while NSP4 showed faster mobility. This distinct electrophoretic behavior was more clearly observed in drug-

217 treated infected cells labeled with ^{3}H-mannose, conditions in which only the two viral
218 glycoproteins are labeled (Fig. 5B).

219 To confirm that the alterations in the electrophoretic mobility of VP7 and NSP4 were due
220 to the inhibition of GBF1, MA104 cells were transfected with the siRNA to GBF1 to
221 silence its expression, and infected with RRV; at 7.5 hpi the cells were pulse-labeled with
222 ^{35}S-Met as described above. As observed when the pharmacological inhibitors were used,
223 knocking down the expression of GBF1 also caused changes in the electrophoretic mobility
224 of VP7 and NSP4 (Fig 5C); in this case, the change was partial, most likely due to
225 incomplete GBF1 knock down in all cells. To our knowledge GBF1 is the first identified
226 regulatory cellular factor that affects the mobility of VP7 and NSP4.

227 Furthermore, we also observed that the modification of the electrophoretic mobility of VP7
228 and NSP4 was independent of the rotavirus strain, since these changes were also observed
229 for rotavirus strains SA11, UK, 69M, and YM, after BFA treatment (data not shown).
230 These results indicate that despite the different amino acid sequences of VP7 and NSP4
231 among the various rotavirus strains, the lack of GBF1 activity inhibits a common
232 posttranslational processing.

233 **Modification of the electrophoretic mobility of VP7 in the presence of BFA or GCA is**
234 **not related to changes in the structure of its carbohydrate chain.** It has been previously
235 shown that the treatment of rotavirus-infected MA104 cells with BFA reduces the
236 electrophoretic mobility of VP7, and it was proposed that this change could be related to an
237 altered oligosaccharide chain (21). To determine if the abnormal migration of VP7 in the
238 presence of the inhibitors was due to a modification of its carbohydrate moiety, we

characterized the effect of the drugs on the migration of the VP7 protein and replication of the mutant strain SA11-CL28, a simian rotavirus SA11 variant that lacks the N-glycosylation site in VP7 and thus is non-glycosylated (51). The absence of glycosylation of this protein was confirmed by metabolically labeling the virus with ^{3}H-mannose. NSP4, but not VP7 was labeled, as detected by PAGE and fluorography (data not shown).

Similar to that observed with wild type SA11 (SA11wt), treatment of cells with BFA or GCA decreased yield of mutant SA11-CL28 virus by more than 90% (Fig. 6A). The drug treatments also reduced the electrophoretic mobility of both, the glycosylated VP7 of SA11wt and the non-glycosylated VP7 of the SA11-CL28 (Fig 6B), suggesting that the change in mobility of VP7 in cells treated with the drugs is not due to a change in glycosylation. Furthermore, by characterizing the electrophoretic mobility of a recombinant RRV VP7 protein overexpressed in MA104 cells, we show that the change observed after BFA treatment is not due to either N- or O-glycosylation or to phosphorylation (Fig. 7A-C). In addition, a recombinant RRV VP7 protein with the N-glycosylation site mutated (69-NST-71 to 69-QSG-71) still showed a reduced electrophoretic mobility after treatment with BFA or GCA, confirming the results observed with the mutant SA11-CL28 virus (Fig.7D).

An inefficient trimerization of VP7 may be responsible for the defective assembly of TLPs. It has been shown that in the absence of VP7 the transiently enveloped intermediate particles do not mature to infectious virus (52); it was proposed that after budding into the lumen of the ER, VP7 assembles into the DLPs excluding the lipid envelope during this process as well as NSP4, yielding the mature infectious virions (52). Since VP7 exists as trimers in the mature, infectious virus particles (17), we evaluated whether BFA and GCA treatments affected trimerization of the protein. For this, MA104 cells were infected with

RRV in the presence of either inhibitor, and 6 hpi the cells were fixed and co-stained with an antibody to the viral nonstructural protein NSP2 that forms part of the viroplasms, and with monoclonal antibody 159 (MAb 159) to VP7, which only recognizes the trimeric form of the protein (18, 53).

In rotavirus-infected, untreated cells, the trimeric isoform of VP7 was observed in the cytoplasm of infected cells, surrounding the viroplasms (Figure 8A). In contrast, in cells treated with BFA or GCA, even though the presence of NSP2 was detected, no signal of the trimeric form of VP7 was observed (Fig 8A). To verify that the lack of trimers was not due to the absence of VP7, we conducted the same assay but using mAb M60, which primarily recognizes the monomeric, non-virion-associated form of VP7 (18, 53). In the absence of inhibitors, the monomeric form of VP7 showed a reticular pattern distributed across the cell cytoplasm, with some of the protein surrounding viroplasms (Figure 8A). Treatment with the inhibitors did not abolish the signal of the VP7 monomers, although the distribution of the protein changed to a punctate pattern (Fig. 8A). Taken together, the treatment with BFA or GCA prevents the formation of VP7 trimers. Of interest, the block in the trimerization of VP7 seems to be independent of alterations in its glycosylation pattern, since BFA also inhibited the trimerization of the VP7 protein of SA11wt and SA11-CL28 viruses without apparently altering the intracellular levels of the monomeric form of the protein (Fig 8B and 8C).

We also found that knocking down the expression of GBF1 abolished the trimerization of VP7 (Fig. 9); similar to the experiments with the pharmacological inhibitors, the trimeric form of VP7 (MAb 159) was detected at 6 hpi in the majority of the infected cells transfected with an irrelevant siRNA. In contrast, in cells transfected with the siRNA to

GBF1, the trimeric form of VP7 could not be detected, even though the cells were positive for NSP2. However, as described above, the absence of trimers was not due to a deficient synthesis of VP7, since in GBF1-silenced cells the monomeric form of VP7 (detected by MAb M60), was observed in most cells (Fig 9).

NSP4 is involved in VP7 trimerization. To explore if the lack of trimerization of VP7 could be related to the change in electrophoretic mobility of NSP4, the expression of NSP4 was silenced by RNAi in MA104 cells stably expressing the NSP5 protein fused to EGFP(54), and the presence of NSP4 as well as the trimeric or monomeric forms of VP7 were determined in infected cells with specific antibodies. As can be observed in Fig 10 (upper panels), cells transfected with an irrelevant siRNA contained the trimeric form of VP7, as detected with Mab159. In contrast, the cells depleted of NSP4 did not show the trimeric form of VP7, even though they were infected as judged by the presence of the viroplasms labeled with NSP5-EGFP. Similar to the previous experiments, the absence of trimers was not due to a deficient synthesis of VP7, since the monomeric form of VP7 (detected with MAb M60) was observed in NSP4-silenced cells (Fig 10, lower panels). Moreover, as previously reported (52), knocking down the expression of NSP4 induced a reduction in the size of viroplasms (Fig 10). This result is consisitent with a previous report showing that NSP4 might stimulate the assembly of VP7 (55).

To further explore whether the trimerization of VP7 depends on the presence of NSP4, Hek293 cells expressing constitutively the T7 polymerase (T7pol) (56) were co-transfected with plasmids D1R and D12L encoding the two subunits of the vaccinia virus capping enzyme, which efficiently caps the T7pol RNA polymerase transcripts in the cytoplasm (57), and with plasmids encoding the NSP4 protein or the non-glycosylated form of VP7, or

with both plasmids simultaneously. At 24 hpt the cells were fixed and immunostained for NSP4 and VP7. In cells in which the plasmid for VP7 was transfected alone, the monomeric form of VP7 (MAb M60) was clearly visible, whereas there was no signal with MAb 159 that detect the trimer; in contrast, when the plasmids for VP7 and NSP4 were co-transfected, trimeric VP7 was detected and colocalized with NSP4 (Fig. 11). These results confirm that the presence of NSP4 is relevant (directly or indirectly) for the correct assembly of VP7 into trimers.

Distinct domains of GBF1 are essential for rotavirus replication. To explore the potential involvement of the different GBF1 domains in rotavirus progeny production, we compared the replication of the virus in Hek293 cells transfected with GBF1 construct containing the A795E mutation (GBF1/795) that confers resistance to BFA (47, 58), or with a series of mutant GBF1/795 proteins (Fig 12A) (59).

For these assays, Hek293 cells were transfected with the different constructs, and at 24 hpt, the cells were infected with RRV. At 12 hpi the total virus was harvested, and the viral yield was determined. Figure 12B shows that the full-length GBF1/795 was able to rescue the replication of rotavirus in the presence of BFA. In addition, the GBF1/795/1531t was able to rescue, albeit partially, viral replication. In contrast, none of the other GBF1 mutants could support virus replication. These findings indicate that the C-terminal domain of GBF1 is not absolutely critical for replication of the virus, while all other domains of GBF1 are required.

We also tested a GBF1/795 mutant that encoded a protein with an amino acid substitution E794K in the Sec7 domain (GBF1/795/E794K) that is inactive in Arf activation (60), and

with a construct in which the C-terminal loop of Sec7 domain (EIVMPEE at positions 883–889) was disrupted by the substitution of 7 alanines, producing a GBF1 protein defective in Arf biding and activation (GBF1/795/7A)(61)(Fig 12A). Both, the catalytic inactive GBF1/795/E794K and GBF1/795/7A mutants were unable to support rotavirus replication in the presence of BFA, suggesting that the ability of GBF1 to activate Arf is important for virus progeny production. All GBF1/795 constructs had been shown to be expressed to a similar level, as determined by western blot (58, 59)

The previous results suggested that Arf1 activation might be important for rotavirus replication. This observation was tested by transfecting MA104 cells with an siRNA to Arf1, which very efficiently knocked-down the synthesis of the protein (Fig. 12C, left), and at 72 hpt, infecting the cells with RRV. At 12 hpi the total virus was harvested, and the viral yield was determined. Silencing the expression of Arf1 did not affect the yield of viral progeny as compared to that produced in cells transfected with a control, irrelevant siRNA (Fig 12C, right). These results suggest that GBF1 catalytic activity is essential for rotavirus replication, but the activation of Arf1 is not required.

DISCUSSION

Eukaryotic cells use elaborated systems to control the traffic of proteins between different organelles. The COPI/Arf1 machinery has been shown to participate in several of these transport processes, including its recent involvement in maturation and function of lipid droplets (LDs) (30–32). The COPI/Arf1 complex is also emerging as an important cellular factor for the replication of several RNA viruses. In the case of influenza (62, 63) and vesicular stomatitis viruses (VSV) (64, 65) the COPI/Arf1 complex seems to play a role in

their entry process. Moreover, for VSV as well as for hepatitis C virus (66–68), mouse hepatitis coronavirus (69), chikungunya virus (70), poliovirus (58, 59, 71), coxsackievirus (72) and classical swine fever virus (73), COPI/Arf1 has been shown to be necessary for genome replication as well as for viral protein expression. COPI/Arf1 has also been shown to be critical for viral particle assembly of influenza and the Chandipura virus (63, 74). The specific mechanism through which COPI/Arf1 participate in these processes has not been characterized; however, GBF1, involved in the first step of the COPI/Arf1 transport process, has been shown to play an important role for the replication of some of these viruses. For example, for enteroviruses, the recruitment of GBF1 to the membranous structures where the viral RNA synthesis takes place, mediated by the viral 3A protein, is crucial for genome replication. Moreover, in this case, the function of GBF1 appears independent of Arf1 activation (58, 75).

In this work, we studied the effect of inhibiting the function of the GBF1/COPI/Arf1 machinery on the replication of rotavirus using the pharmacological inhibitors BFA and GCA. We found that both inhibitors induced a significant reduction in the progeny production of different rotavirus strains belonging to different G and P serotypes, indicating that these drugs block a common pathway for all these viruses.

GCA inhibits the COPI/Arf1 machinery activity by selectively inhibiting GBF1; BFA, on the other hand, also inhibits BIG1 and BIG2 (49, 76). BIG1 and BIG2 are involved in vesicular traffic of clathrin-coated vesicles at the TGN (77–79). Our observations suggest that GBF1, and not the BIGs, is the factor targeted by BFA and GCA that causes the reduction of rotavirus replication. The importance of GBF1 was confirmed since knocking down the expression of GBF1 by RNAi decreased the infectivity of RRV by about 70%.

375 In line with previous observations, we found that in cells treated with BFA and infected
376 with RRV, the electrophoretic mobility of both VP7 and NSP4 was modified. Although it
377 has been clearly demonstrated that the modification of NSP4 is due to oligosaccharide
378 processing (21), the modification of VP7 is currently unknown. Since no infectious virus
379 was produced under those conditions, it was also proposed that the altered oligosaccharide
380 processing of VP7 was responsible for the defective assembly of viral particles (21). Our
381 results indicate that for VP7, the altered electrophoretic mobility is independent of its
382 glycosylation pattern, since both the non-glycosylated VP7 of the SA11-CL28 virus and a
383 recombinant VP7 protein with the N-glycosylation site mutated showed an altered mobility
384 in the presence of the drugs. These results are in agreement with previous findings showing
385 that cell treatment with both BFA and tunicamycin, an inhibitor of N-glycosylation (80),
386 produce a VP7 protein with altered mobility (21). In addition, the changes in VP7 mobility
387 were not due to O-glycosylation nor phosphorylation of the protein. The possibility that the
388 drugs block the removal of the signal peptide of VP7 (81) remains to be explored.

389 The observation that silencing the expression of GBF1 induced changes in the mobility of
390 both VP7 and NSP4 suggests that the activity of this cellular factor is essential for the
391 correct processing of both proteins. Taking into consideration that GBF1 functions at the
392 ER-Golgi interface and that rotaviruses mature in the ER, it seems likely that Golgi-ER
393 transport is the relevant process required for the correct maturation of rotavirus infectious
394 particles. However, considering that LDs have been proposed to play a significant role in
395 the replication cycle of rotaviruses, it remains possible that the protein transport between
396 the ER membrane and LDs is needed for the correct processing of both VP7 (glycosylation
397 independent) and NSP4. However, an unknown function of GBF1 cannot be discarded.

Since the assembly of VP7 onto DLPs has been suggested to require VP7 trimerization, the effect of the drugs on trimerization was evaluated. We found that VP7 was not able to trimerize (as judged by the lack of recognition of VP7 by MAb 159, which specifically interacts with the trimeric but not with the monomeric form of the protein (18)) in the presence of the inhibitors or in cells where the GBF1 expression was silenced,. Our findings differ from previous observations that BFA has minimal effects on the antigenicity of VP7 (as judged by recognition by MAb 159 in immunoperoxidase staining (21)). The reason for this discrepancy might be the methods employed for the detection of the MAb159 signal, immunofluorescence in our work versus immunoperoxidase staining in the previous report (21), which may have different sensitivity.

The drug-induced modification of VP7 could, in principle, prevent its trimerization. However, it is also possible that the modification of NSP4 could impair VP7 trimerization. Even if the NSP4 function as a receptor in the ER membrane is not affected by the drug treatments, it is plausible that the modifications in its glycosylation pattern could affect its role in facilitating (directly or indirectly) the trimerization of VP7 during the removal of the envelope in the last step virus assembly. The role of NSP4 in the trimerization of VP7 is supported by earlier observation where tunicamycin, an inhibitor of N-glycosylation, restricts the maturation of enveloped particles of SA11-CL28 by inhibiting the glycosylation of NSP4 (82). On the other hand, it is known that the stability of the VP7 trimers depends on the presence of calcium (Ca2+) (15, 18), suggesting that alteration in the calcium homeostasis of the cell could be responsible for the lack of the outer layer assembly of rotaviruses. It has been shown that rotavirus infection increases the Ca2+ permeability of the plasma membrane, leading to an enhancement of its intracellular

concentration, but that BFA inhibits this enhancement (83). Thus, it cannot be excluded that the deficient trimerization of VP7 is due to altered calcium homeostasis.

The multidomain structure of GBF1 allows it to engage in numerous interactions with other cellular, as well as viral proteins (33, 59, 75). To gain information about the importance of the different domains of GBF1 in rotavirus replication, we tested the ability of different truncated forms of GBF1 to support the production of virus progeny in the presence of BFA. A recombinant full length GBF1 carrying a mutation in the Sec7 domain that renders the protein resistant to the inhibitory action of BFA (GBF1/795) was able to rescue virus replication, as did a mutant GFB1 protein lacking the C-terminal HDS3 domain (albeit less well), suggesting that HDS3 is dispensable for viral replication. Although the precise function of the HDS3 is unknown, it appears essential for GBF1 membrane association, since the GBF1/795/1531t mutant is inefficiently targeted to Golgi, remaining predominantly cytosolic, albeit some fraction of this mutant is able to associate the membranes (unpublished results). It possible that the small fraction of the GBF1/795/1531t mutant that is able to associate to membranes is capable to activate sufficient Arf molecules to allow the lifecycle of the virus to proceed.

The catalytically inactive mutants of GBF1 (GBF1/795/E794K and GBF1/795/7A) failed to support replication of the virus, suggesting that GBF1 activity is essential for rotavirus progeny production. Although the catalytic activity of GBF1 appears essential for rotavirus replication, we found that the activation of Arf1 is not required, since knocking- down the expression of this factor does not affect the production of infectious virus. Thus, it is likely that rotavirus replication requires the activation of other GBF1 substrates, such as Arf4 or

443 Arf5 (Claude et al., 1999; Niu et al., 2005; Szul et al., 2005) that could compensate for the
444 reduced level of Arf1.

445 Previous findings reported that the most N-terminal 37 amino acids of GBF1 are important
446 for the replication of coxsackie B3 virus and poliovirus (58, 59, 75, 84) by targeting the 3A
447 protein to membranes where the virus replication complexes will assemble. Similarly, we
448 showed that this deletion renders GBF1 unable to support rotavirus replication in the
449 presence of BFA. It is possible that this 37 amino acid stretch could bind a rotaviral protein,
450 although it may also interact with a cellular factor to support virus replication. In fact, it has
451 been reported that Rab1b is able to interact with the N-terminus of GBF1 to modulate
452 GBF1 function in the secretory pathway (85). Further experiments will have to be carried
453 out to explore more in detail the mechanism through which GBF1 supports rotavirus
454 replication.

455 **MATERIALS AND METHODS**

456 **Cell and viruses.** MA104 rhesus monkey kidney epithelial cells (ATCC), and Hek293
457 human embryonic cells stably expressing phage T7 polymerase, kindly provided by Dr.
458 Carlos Sandoval Jaime (Instituto de Biotecnología, Cuernavaca, Mexico) (56), were grown
459 in Dulbecco's Modified Eagle Medium-Reduced Serum (DMEM-RS) (Thermo Scientific
460 HyClone, Logan, UT) supplemented with 5% heat-inactivated fetal bovine serum (FBS)
461 (Biowest, Kansas City, MO) at 37°C in a 5% CO2 atmosphere. Simian (RRV, G3P5B[3];
462 SA11, G3P5B[2]; and SA11-CL28, G3P5B[2]), bovine (UK, G6P7[5]), porcine (YM,
463 G11P9[7]), and human (69M, G8P4[10]) rotaviruses were propagated in MA104. Briefly,
464 the viruses were activated with trypsin (10 µg/ml; Gibco, Life Technologies, Carlsbad, CA,

465 USA) for 30 min at 37°C. Afterwards, the activated viruses were adsorbed to the cells for 1
466 h at 37°C. The unbound virus was removed, and the cells were incubated for 16 h at 37 °C.
467 Finally, the cells were lysed by two cycles of freeze-thawing and the cell debris were
468 removed by centrifugation. The resulting viral lysate was stored at -70°C.

469 **Reagents and antibodies.** Brefeldin A (B7651, Sigma-Aldrich, St. Louis, MO, USA) was
470 dissolved in ethanol, and Golgicide A (345862, Calbiochem, San Diego, CA, USA) was
471 dissolved in dimethyl sulfoxide (DMSO). Monoclonal antibodies (MAbs) to the monomeric
472 (M60) and trimeric (MAb159) forms of VP7 (53) were kindly provided by H. B. Greenberg
473 (Stanford University, Stanford, USA). The rabbit anti-rotavirus polyclonal serum raised
474 against purified TLPs(52), the rabbit polyclonal sera to NSP2(86) and NSP4(87), as well as
475 the rabbit polyclonal sera to human vimentin(52), were produced in our laboratory. Mouse
476 monoclonal antibody to GBF1 was purchased from BD Transduction Laboratories (San
477 Jose, CA, USA). Goat anti-mouse Alexa-488, goat anti-mouse Alexa-647, and goat anti-
478 rabbit Alexa-568-conjugated used as secondary antibodies were obtained from Molecular
479 Probes (Eugene, OR, USA). Horseradish peroxidase-conjugated goat anti-rabbit and anti-
480 mouse antibodies were purchased from PerkinElmer Life Sciences (Boston, MA, USA).

481 **SiRNAs and plasmids.** The small interfering RNA (siRNA) to GBF1, Arf1 and the control
482 siGENOME nontargeting siRNA were purchased from GE Healthcare Dharmacon
483 (Lafayette, CO, USA). For the construction of pcDNA3-VP7 and pcDNA3-NSP4 plasmids,
484 the VP7 and NSP4 genes were cloned from extracts of RRV- and SA11-infected cells,
485 respectively. The cDNA was obtained by RT-PCR using specific primers for amplifying
486 the open reading frame (ORF) of VP7 or NSP4 and cloned into pcDNA3 (Life
487 Technologies, USA) as KpnI-EcoRI fragments. The pcDNA3-non glycosylated VP7

plasmid was obtained by site-direct mutagenesis of the glycosylated VP7 of RRV. Vaccinia virus capping enzyme expression plasmids, pCAG-D1R and pCAG-D12L (Addgene plasmids # 89160 and # 89161, respectively) were a gift from T. Kobayashi (Osaka University, Osaka, Japan). All GBF1 (UniProtKB: Q92538) truncations were introduced into the backbone of Venus tagged-GBF1/A795E (described in 57) using QuickChange XL site-directed mutagenesis kit from Agilent Technology. The GBF1/795/E794K construct was generated by introducing the A795E mutation into GFP-tagged GBF1 E794K-GFP construct (described in 59). Following PCR, constructs were transformed into XL 10 gold cells. DNA was isolated and all mutations were confirmed by sequencing. The GBF1/795/7A construct has been described (61). The GBF11/795/Δ37 construct has been described (58).

Immunoperoxidase assay. MA104 cells were grown in 96-well plates to confluence. The cells were then infected with two-fold serial dilutions of the different viral lysates for 1h at 37°C. After this time, the non-adsorbed virus was removed, and the cells were incubated at 37°C for 16 h. Afterwards, the cells were fixed with 80% acetone in phosphate-buffered saline (PBS) for 30 min at room temperature and then washed twice with PBS. The fixed monolayers were then incubated with a rabbit anti-rotavirus polyclonal serum, followed by incubation with a secondary anti-rabbit antibody conjugated with horseradish peroxidase. Finally, the cells were washed twice with PBS and stained with a solution of 1 mg/ml of carbazole (AEC) in sodium acetate buffer (50 mM, pH 5) with 0.04% H_2O_2. The reaction was stopped by washing in tap water, and the infectious focus forming units were counted in a Nikon TMS Inverted Phase Contrast Microscope with a 20X objective.

510 **Transfection of siRNAs and plasmids**. Transfection of siRNAs into MA104 cells was
511 performed with Oligofectamine reagent (Invitrogen, Carlsbad, CA, USA) in 48-well plates
512 using a reverse transfection method as described previously (88). Plasmids were transfected
513 either into MA014 cells or Hek293 cells constitutively expressing the T7 polymerase, using
514 Lipofectamine 3000 (Invitrogen, Carlsbad, CA, USA) according to the manufacturer's
515 instructions.

516 **Enrichment of viral particles.** RRV (at an MOI of 5) was adsorbed to MA104 cells for 1 h
517 at 4°C to allow the virus to bind to the cells. The unbound virus was removed, and the cells
518 were incubated at 37 °C to allow the infection to proceed. At different times post-infection
519 cells were washed with EGTA (3 mM) for 5s to release any viral particles that remained
520 bound to the cell surface, and the cells were lysed by freeze-thawing. Viral lysates were
521 centrifuged at 105,000 x g for 1h at 4°C in a 45Ti rotor using a Beckman ultracentrifuge
522 (OptimaL-90). The supernatant was discarded and the viral particles in the pellet were
523 resuspended in 4 ml TNC buffer (10 mM Tris, pH7.5, 140 mM NaCl, 10 mM $CaCl_2$),
524 extracted with trichloromonofluoromethane (Genetron, CYDSA 11, Mexico City, Mexico)
525 and placed on top of a 1 ml 40% sucrose cushion in TNC. The samples were centrifuged at
526 195,000 x g for 2 h at 4°C in a SW55Ti rotor. Finally, the resulting pellets containing the
527 semi-purified viral particles were dissolved in TNC and analyzed by SDS-PAGE.

528 **Isopycnic gradient.** MA104 cells were infected with RRV at an MOI of 5 in the presence
529 of either 0.5 µg/ml BFA or 10µM GCA, and at 12 hpi the cells were lysed by freeze-
530 thawing. The cell lysate was extracted with trichloromonofluoromethane as described
531 above, and the aqueous phase was mixed with 2.2 g of CsCl and TNC buffer up to 5 ml.
532 The samples were centrifuged at 158,000 x g for 18h at 4°C on a SW55Ti rotor (Beckman).

533 Finally, the opalescent bands corresponding to TLPs and DLPs were collected by puncture
534 with a syringe and stored at 4°C. Before use, the viral particles were desalted in a Sephadex
535 G25 spin column.

536 **Transmission electron microscopy.** MA104 cells were seeded onto sapphire discs and
537 infected with RRV an MOI of 250 viroplasm forming units (VFU)/ml in the presence of 0.5
538 µg/ml BFA or 10µM GCA. At 6 hpi the cells were fixed with 2.5% glutaraldehyde in 100
539 mM Na/K-phosphate buffer, pH 7.4 for 1 h at 4˚C and kept in 100 mM Na/K-phosphate
540 buffer overnight at 4˚C. Afterwards, samples were post-fixed in 1% osmium tetroxide in
541 100 mM Na/K-phosphate buffer for 1 h at 4˚C, dehydrated in a graded ethanol series
542 starting at 70% followed by two changes in acetone and embedded in Epon. Ultrathin
543 sections (60-80 nm) were cut and stained with uranyl acetate and lead citrate. Images were
544 acquired using a transmission electron microscope (CM12, Philips, Eindhoven, The
545 Netherlands) equipped with a CCD camera (Ultrascan 1000, Gatan, Pleasanton, CA, USA)
546 at an acceleration of 100kV and processed using ImageJ version 2.0.0-rc-69/1.52i (Creative
547 Common, http://imageJ.net/contributors).

548 **Metabolic labeling of proteins.** MA104 cells were pre-treated with BFA (0.5 µg/ml) or
549 GCA (10 µM) for 30 min. Afterwards, the cells were mock-infected or infected with RRV
550 (MOI of 5) in the presence of inhibitors for 1h. At the end of the adsorption period, the cells
551 were washed, and fresh media containing the drugs were added. At 7 hpi, the cells were
552 starved for 30 min in the methionine-free medium before pulse-labeling with 25 µCi/ml of
553 Easy Tag Express ^{35}S labeling mix (Perkin Elmer, Shelton, CT, USA) for 30 min. At 8 hpi,
554 cells were washed three times, and the monolayers were incubated in complete medium

555 before lysis in Laemmli sample buffer at 10 hpi. The radiolabeled proteins were resolved in
556 a 10% SDS-PAGE, followed by autoradiography.

557 For ^{3}H-mannose radiolabeling, cells were treated and infected as described above. At 6 hpi
558 the cells were starved in a glucose-free medium for 30 min followed by labeling with 200
559 µCi/ml of mannose-D-[2-^{3}H(N)] (Perkin Elmer, Shelton, CT) for 1.5 h. At 8 hpi, the ^{3}H-
560 labelling medium was removed, and the cells were incubated in complete medium before
561 lysis in Laemmli sample buffer at 10 hpi. The radiolabeled proteins were resolved by 10%
562 SDS-PAGE, followed by fluorography.

563 **Western blot analysis.** Proteins in cell lysates were separated in a SDS-PAGE and
564 transferred to Immobilon NC (Millipore Merck, Darmstadt, Germany) membranes. The
565 membranes were blocked with 5% nonfat dry milk in PBS for 1 h at room temperature and
566 then incubated with primary antibodies diluted in PBS containing 0.1% nonfat dry milk.
567 The membranes were then incubated with the corresponding secondary antibody
568 conjugated to horseradish peroxidase. The peroxidase activity was developed using the
569 Western Lightning Chemiluminescence Reagent Plus (PerkinElmer) according to the
570 manufacturer's instructions. The blots were also probed with an anti-vimentin antibody,
571 which was used as a loading control.

572 **Endoglycosidases and phosphatase treatments.** The pcDNA3-VP7 plasmid was
573 transfected in MA104 cells; BFA or GCA (5 µg/ml) were added at 1 hpt and the cells were
574 lysed (7.6% SDS, 125 mM TrisHCl, pH 6.8) at 18 hpt. Cell extracts underwent treatment
575 with either of the following enzymes according to the manufacturer instructions (Life

576 Technologies, Carlsbad, CA, USA): PNGaseF (Peptide-N-Glycosidase F), EndoH (endo-β-
577 N-acetylglucosaminidase-H), a Protein Deglycosylation Mix, and λ-phospatase.

578 **Immunofluorescence**. MA104 cells grown on glass coverslips were pre-treated with BFA
579 (0.5 µg/ml) or GCA (10 µM) for 30 min and then infected with rotavirus at an MOI of 1.
580 Six hpi, cells were fixed with 2% paraformaldehyde in PBS for 20 min at room
581 temperature. After this time, the cells were washed four times with 50 mM NH_4Cl in PBS
582 and permeabilized by incubation with 0.5% Triton X-100 for 15 min at room temperature.
583 The coverslips were incubated in blocking buffer (1% bovine serum albumin) for 1h at
584 room temperature (RT) and then with primary antibodies diluted in blocking buffer
585 overnight at 4°C. The cells were then washed five times and incubated with the Alexa-
586 labeled secondary antibodies in blocking buffer for 1 h at RT. Finally, cell nuclei were
587 stained with 30 nM DAPI (4′,6-diamidino-2-phenylindole, Invitrogen, Eugene, OR, USA)
588 for 5 min and the coverslips were mounted onto glass slides with CitiFluor AF1 antifading
589 (Electron Microscopy Sciences, Emsdiasum, Hatfield Penn). Images were acquired with an
590 inverted 3I spinning disk confocal microscope (Zeiss Observer Z.1) coupled to a digital
591 EMCCD Andor Ixon (512x512 pixels) and processed using Fiji ImageJ 1.52n(89).

592 **Statistical analysis**. Statistical significance was evaluated by the Mann–Whitney–
593 Wilcoxon test using GraphPad Prism 8.0.2. (GraphPad Software Inc.). The homogeneity of
594 variances was confirmed by a Fligner Killeen test using R 3.6.0.

595 **ACKNOWLEDGMENTS**

596 J.L.M. is recipient of a scholarship from CONACyT. This work was partially supported by
597 grant IG200317 from DGAPA/UNAM, by grant A1-5-15356 from the National Council for

Science and Technology, Conacyt-Mexico, and by the University of Zurich. The funders had no role in study design, data collection, and interpretation, or the decision to submit the work for publication.

REFERENCES

1. Estes M, Greenberg H. 2007. Rotaviruses, p. 1347–1401. In Fields, BN, Knipe, DM Howley PM (ed), Fields of Virology, 6th ed, vol 2. Wolters Kluwer Health/Lippincott Williams & Wilkins, Philadelphia, PA.
2. Trask SD, McDonald SM, Patton JT. 2012. Structural insights into the coupling of virion assembly and rotavirus replication. Nat Rev Microbiol 10:165–177.
3. Patton JT, Silvestri LS, Tortorici MA, Vasquez-Del Carpio R, Taraporewala ZF. 2006. Rotavirus genome replication and morphogenesis: role of the viroplasm. Curr Top Microbiol Immunol 309:169–87.
4. Patton JT, Vasquez-Del Carpio R, Tortorici MA, Taraporewala ZF. 2006. Coupling of Rotavirus Genome Replication and Capsid Assembly. Adv Virus Res 69:167–201.
5. Chasey D. 1977. Different particle types in tissue culture and intestinal epithelium infected with rotavirus. J Gen Virol 37:443–451.
6. Poruchynsky MS, Atkinson PH. 1991. Rotavirus protein rearrangements in purified membrane-enveloped intermediate particles. J Virol 65:4720–4727.
7. Both GW, Siegman LJ, Bellamy AR, Atkinson PH. 1983. Coding assignment and nucleotide sequence of simian rotavirus SA11 gene segment 10: location of glycosylation sites suggests that the signal peptide is not cleaved. J Virol 48:335–9.
8. Au KS, Mattion NM, Estes MK. 1993. A subviral particle binding domain on the rotavirus nonstructural glycoprotein ns28. Virology 194:665-673.
9. Au KS, Chan WK, Burns JW, Estes MK. 1989. Receptor activity of rotavirus nonstructural glycoprotein NS28. J Virol 63:4553–62.
10. O'Brien JA, Taylor JA, Bellamy AR. 2000. Probing the structure of rotavirus NSP4: a short sequence at the extreme C terminus mediates binding to the inner capsid particle. J Virol 74:5388–94.
11. Maass, D; Atkinson PH. 1990. Rotavirus Proteins VP7, NS28, and VP4 Form Oligomeric Structures. J Virol 64:2632–2641.
12. Bergmann CC, Maass D, Poruchynsky MS, Atkinson PH, Bellamy AR. 1989. Topology of the non-structural rotavirus receptor glycoprotein NS28 in the rough endoplasmic reticulum. EMBO J 8:1695–1703.

13. Petrie BL, Graham DY, Estes MK. 1981. Identification of Rotavirus Particle Types. Intervirology 16:20–28.
14. Suzuki H, Konno T, Numazaki Y. 1993. Electron microscopic evidence for budding process-independent assembly of double-shelled rotavirus particles during passage through endoplasmic reticulum membranes. J Gen Virol 74:2015–2018.
15. Yeager M, Dryden KA, Olson NH, Greenberg HB, Baker TS. 1990. Three-dimensional structure of rhesus rotavirus by cryoelectron microscopy and image reconstruction. J Cell Biol 110:2133–44.
16. Crawford SE, Mukherjee SK, Estes MK, Lawton JA, Shaw AL, Ramig RF, Prasad B V. 2001. Trypsin cleavage stabilizes the rotavirus VP4 spike. J Virol 75:6052–61.
17. Aoki ST, Settembre EC, Trask SD, Greenberg HB, Harrison SC, Dormitzer PR. 2009. Structure of rotavirus outer-layer protein VP7 bound with a neutralizing Fab. Science 324:1444–7.
18. Dormitzer PR, Greenberg HB, Harrison SC. 2000. Purified recombinant rotavirus VP7 forms soluble, calcium-dependent trimers. Virology 277:420–8.
19. Silva-Ayala D, Lopez T, Gutierrez M, Perrimon N, Lopez S, Arias CF. 2013. Genome-wide RNAi screen reveals a role for the ESCRT complex in rotavirus cell entry. Proc Natl Acad Sci 110:10270–10275.
20. Green VA, Pelkmans L. 2016. A Systems Survey of Progressive Host-Cell Reorganization during Rotavirus Infection. Cell Host Microbe 20:107–120.
21. Mirazimi A, Von Bonsdorff CH, Svensson L. 1996. Effect of Brefeldin a on rotavirus assembly and oligosaccharide processing. Virology 217:554–563.
22. Popoff V, Adolf F, Brugger B, Wieland F. 2011. COPI Budding within the Golgi Stack. Csh Perspect Biol 3:a005231–a005231.
23. Griffiths G, Pepperkok R, Locker JK, Kreis TE. 1995. Immunocytochemical localization of beta-COP to the ER-Golgi boundary and the TGN. J Cell Sci 108:2839–2856.
24. Duden R, Griffiths G, Frank R, Argos P, Kreis TE. 1991. Beta-COP, a 110 kd protein associated with non-clathrin-coated vesicles and the Golgi complex, shows homology to beta-adaptin. Cell 64:649–65.
25. Gu F, Aniento F, Parton RG, Gruenberg J. 1997. Functional Dissection of COP-I Subunits in the Biogenesis of Multivesicular Endosomes. J Cell Biol 139:1183–1195.
26. Daro E, Sheff D, Gomez M, Kreis T, Mellman I. 1997. Inhibition of endosome function in CHO cells bearing a temperature-sensitive defect in the coatomer (COPI) component epsilon-COP. J Cell Biol 139:1747–59.
27. Botelho RJ, Hackam DJ, Schreiber AD, Grinstein S. 2000. Role of COPI in Phagosome Maturation. J Biol Chem 275:15717–15727.

28. Razi M, Chan EYW, Tooze SA. 2009. Early endosomes and endosomal coatomer are required for autophagy. J Cell Biol 185:305–321.
29. Lay D, Gorgas K, Just WW. 2006. Peroxisome biogenesis: Where Arf and coatomer might be involved. BBA - Mol Cell Res 1763:1678–1687.
30. Beller M, Sztalryd C, Southall N, Bell M, Jäckle H, Auld DS, Oliver B. 2008. COPI complex is a regulator of lipid homeostasis. PLoS Biol 6:2530–2549.
31. Guo Y, Walther TC, Rao M, Stuurman N, Goshima G, Terayama K, Wong JS, Vale RD, Walter P, Farese R V. 2008. Functional genomic screen reveals genes involved in lipid-droplet formation and utilization. Nature 453:657–661.
32. Wilfling F, Thiam AR, Olarte M-J, Wang J, Beck R, Gould TJ, Allgeyer ES, Pincet F, Bewersdorf J, Farese R V, Walther TC. 2014. Arf1/COPI machinery acts directly on lipid droplets and enables their connection to the ER for protein targeting. Elife 3:e01607.
33. Kaczmarek B, Verbavatz JM, Jackson CL. 2017. GBF1 and Arf1 function in vesicular trafficking, lipid homoeostasis and organelle dynamics. Biol Cell 109:391-399.
34. Hsu VW, Yang J-S. 2009. Mechanisms of COPI vesicle formation. FEBS Lett 583:3758–3763.
35. Beck R, Ravet M, Wieland FT, Cassel D, Cassel D. 2009. The COPI system: Molecular mechanisms and function. FEBS Lett 583:2701–2709.
36. Anders N, Jürgens G. 2008. Large ARF guanine nucleotide exchange factors in membrane trafficking. Cell Mol Life Sci 65:3433-3445.
37. Claude A, Zhao B-P, Kuziemsky CE, Dahan S, Berger SJ, Yan J-P, Armold AD, Sullivan EM, Melançon P. 1999. GBF1: A Novel Golgi-associated BFA-resistant Guanine Nucleotide Exchange Factor That Displays Specificity for ADP-ribosylation Factor 5. J Cell Biol 146:71–84.
38. Niu T, Pfeifer AC, Lippincott-schwartz J, Jackson CL. 2005. Dynamics of GBF1 , a Brefeldin A-Sensitive Arf1 Exchange Factor at the Golgi. Mol Biol Cell 16:1213–1222.
39. Szul T, Garcia-Mata R, Brandon E, Shestopal S, Alvarez C, Sztul E. 2005. Dissection of membrane dynamics of the ARF-guanine nucleotide exchange factor GBF1. Traffic 6:374–385.
40. Morinaga N, Adamik R, Moss J, Vaughan M. 1999. Brefeldin A inhibited activity of the sec7 domain of p200, a mammalian guanine nucleotide-exchange protein for ADP-ribosylation factors. J Biol Chem 274:17417–23.
41. Togawa A, Morinaga N, Ogasawara M, Moss J, Vaughan M. 1999. Purification and cloning of a brefeldin A-inhibited guanine nucleotide-exchange protein for ADP-ribosylation factors. J Biol Chem 274:12308–12315.
42. Shin H-W, Morinaga N, Noda M, Nakayama K. 2004. BIG2, A Guanine Nucleotide Exchange Factor for ADP-Ribosylation Factors: Its Localization to

Recycling Endosomes and Implication in the Endosome Integrity. Mol Biol Cell 15:5283–5294.

43. Ramaen O, Joubert A, Simister P, Belgareh-Touzé N, Olivares-Sanchez MC, Zeeh J-C, Chantalat S, Golinelli-Cohen M-P, Jackson CL, Biou V, Cherfils J. 2007. Interactions between Conserved Domains within Homodimers in the BIG1, BIG2, and GBF1 Arf Guanine Nucleotide Exchange Factors. J Biol Chem 282:28834–28842.

44. Bhatt JM, Viktorova EG, Wyrozumska P, Lin H, Belov GA, Busby T, Kahn RA, Sztul E, Wright J, Lee E, Newman LE. 2015. Oligomerization of the Sec7 domain Arf guanine nucleotide exchange factor GBF1 is dispensable for Golgi localization and function but regulates degradation. Am J Physiol Physiol 310:C456–C469.

45. Bouvet S, Golinelli-Cohen M-P, Contremoulins V, Jackson CL. 2013. Targeting of the Arf-GEF GBF1 to lipid droplets and Golgi membranes. J Cell Sci 126:4794–4805.

46. Ellong EN, Soni KG, Bui QT, Sougrat R, Golinelli-Cohen MP, Jackson CL. 2011. Interaction between the triglyceride lipase ATGL and the arf1 activator GBF1. PLoS One 6:e21889.

47. Meissner JM, Bhatt JM, Lee E, Styers ML, Ivanova AA, Kahn RA, Sztul E. 2018. The ARF guanine nucleotide exchange factor GBF1 is targeted to Golgi membranes through a PIP-binding domain. J Cell Sci 131:jcs210245.

48. Chen J, Wu X, Yao L, Yan L, Zhang L, Qiu J, Liu X, Jia S, Meng A. 2017. Impairment of cargo transportation caused by gbf1 mutation disrupts vascular integrity and causes hemorrhage in zebrafish embryos. J Biol Chem 292:2315–2327.

49. Sáenz JB, Sun WJ, Chang JW, Li J, Bursulaya B, Gray NS, Haslam DB. 2009. Golgicide A reveals essential roles for GBF1 in Golgi assembly and function. Nat Chem Biol 5:157–165.

50. Mossessova E, Corpina RA, Goldberg J. 2003. Crystal structure of ARF1*Sec7 complexed with Brefeldin A and its implications for the guanine nucleotide exchange mechanism. Mol Cell 12:1403–11.

51. Estes MK, Graham DY, Ramig RF, Ericson BL. 1982. Heterogeneity in the structural glycoprotein (VP7) of simian rotavirus SA11. Virology 122:8–14.

52. Lopez T, Camacho M, Zayas M, Najera R, Sanchez R, Arias CF, Lopez S. 2005. Silencing the Morphogenesis of Rotavirus. J Virol 79:184–192.

53. Shaw RD, Vo PT, Offit PA, Coulsont BS, Greenberg HB. 1986. Antigenic mapping of the surface proteins of rhesus rotavirus. Virology 155:434–451.

54. Eichwald C, Rodriguez JF, Burrone OR. 2004. Characterization of rotavirus NSP2/NSP5 interactions and the dynamics of viroplasm formation. J Gen Virol 85:625–634.

55. Cuadras MA, Bordier BB, Zambrano JL, Ludert JE, Greenberg HB. 2006. Dissecting Rotavirus Particle-Raft Interaction with Small Interfering RNAs: Insights into Rotavirus Transit through the Secretory Pathway. J Virol 80:3935–3946.
56. Sandoval-Jaime C, Green KY, Sosnovtsev S V. 2015. Recovery of murine norovirus and feline calicivirus from plasmids encoding EMCV IRES in stable cell lines expressing T7 polymerase. J Virol Methods 217:1–7.
57. Kanai Y, Komoto S, Kawagishi T, Nouda R, Nagasawa N, Onishi M, Matsuura Y, Taniguchi K, Kobayashi T. 2017. Entirely plasmid-based reverse genetics system for rotaviruses. Proc Natl Acad Sci 114:2349–2354.
58. Belov GA, Feng Q, Nikovics K, Jackson CL, Ehrenfeld E. 2008. A critical role of a cellular membrane traffic protein in poliovirus RNA replication. PLoS Pathog 4:e1000216.
59. Belov GA, Kovtunovych G, Jackson CL, Ehrenfeld E. 2010. Poliovirus replication requires the N-terminus but not the catalytic Sec7 domain of ArfGEF GBF1. Cell Microbiol 12:1463–1479.
60. García-Mata R, Szul T, Alvarez C, Sztul E. 2003. ADP-ribosylation factor/COPI-dependent events at the endoplasmic reticulum-Golgi interface are regulated by the guanine nucleotide exchange factor GBF1. Mol Biol Cell 14:2250–61.
61. Lowery J, Szul T, Seetharaman J, Jian X, Su M, Forouhar F, Xiao R, Acton TB, Montelione GT, Lin H, Wright JW, Lee E, Holloway ZG, Randazzo PA, Tong L, Sztul E. 2011. Novel C-terminal motif within Sec7 domain of guanine nucleotide exchange factors regulates ADP-ribosylation factor (ARF) binding and activation. J Biol Chem 286:36898–36906.
62. König R, Stertz S, Zhou Y, Inoue A, Hoffmann H-H, Bhattacharyya S, Alamares JG, Tscherne DM, Ortigoza MB, Liang Y, Gao Q, Andrews SE, Bandyopadhyay S, De Jesus P, Tu BP, Pache L, Shih C, Orth A, Bonamy G, Miraglia L, Ideker T, García-Sastre A, Young JAT, Palese P, Shaw ML, Chanda SK. 2010. Human host factors required for influenza virus replication. Nature 463:813–817.
63. Sun E, He J, Zhuang X. 2013. Dissecting the Role of COPI Complexes in Influenza Virus Infection. J Virol 87:2673–2685.
64. Cureton DK, Burdeinick-Kerr R, Whelan SPJ. 2012. Genetic inactivation of COPI coatomer separately inhibits vesicular stomatitis virus entry and gene expression. J Virol 86:655–66.
65. Irurzun A, Pérez L, Carrasco L. 1993. Brefeldin A blocks protein glycosylation and RNA replication of vesicular stomatitis virus. FEBS Lett 336:496–500.
66. Goueslain L, Alsaleh K, Horellou P, Roingeard P, Descamps V, Duverlie G, Ciczora Y, Wychowski C, Dubuisson J, Rouille Y. 2010. Identification of GBF1

as a Cellular Factor Required for Hepatitis C Virus RNA Replication. J Virol 84:773–787.

67. Farhat R, Goueslain L, Wychowski C, Belouzard S, Fénéant L, Jackson CL, Dubuisson J, Rouillé Y. 2013. Hepatitis C Virus Replication and Golgi Function in Brefeldin A-Resistant Hepatoma-Derived Cells. PLoS One 8:10–12.

68. Lebsir N, Goueslain L, Farhat R, Callens N, Dubuisson J, Jackson CL, Rouillé Y. 2018. Functional and physical interaction between the Arf activator GBF1 and hepatitis C virus NS3 protein. J Virol 93:e01459-18.

69. Verheije MH, Raaben M, Mari M, Te Lintelo EG, Reggiori F, van Kuppeveld FJM, Rottier PJM, de Haan CAM. 2008. Mouse hepatitis coronavirus RNA replication depends on GBF1-mediated ARF1 activation. PLoS Pathog 4:e1000088.

70. Zhang N, Zhang L. 2017. Key components of COPI and COPII machineries are required for chikungunya virus replication. Biochem Biophys Res Commun 493:1190–1196.

71. Belov GA, Ehrenfeld E. 2007. Involvement of cellular membrane traffic proteins in poliovirus replication. Cell Cycle 6:36–38.

72. Lanke KHW, van der Schaar HM, Belov GA, Feng Q, Duijsings D, Jackson CL, Ehrenfeld E, van Kuppeveld FJM. 2009. GBF1, a Guanine Nucleotide Exchange Factor for Arf, Is Crucial for Coxsackievirus B3 RNA Replication. J Virol 83:11940–11949.

73. Liang W, Zheng M, Bao C, Zhang Y. 2017. CSFV proliferation is associated with GBF1 and Rab2. J Biosci 42:43–56.

74. Rajasekharan S, Rana J, Gulati S, Sharma SK, Gupta V, Gupta S. 2013. Predicting the host protein interactors of Chandipura virus using a structural similarity-based approach. Pathog Dis 69:29–35.

75. Wessels E, Duijsings D, Lanke KHW, Melchers WJG, Jackson CL, van Kuppeveld FJM. 2007. Molecular determinants of the interaction between coxsackievirus protein 3A and guanine nucleotide exchange factor GBF1. J Virol 81:5238–45.

76. Shen X, Xu K-F, Fan Q, Pacheco-Rodriguez G, Moss J, Vaughan M. 2006. Association of brefeldin A-inhibited guanine nucleotide-exchange protein 2 (BIG2) with recycling endosomes during transferrin uptake. Proc Natl Acad Sci 103:2635–2640.

77. Donaldson JG, Jackson CL. 2011. ARF family G proteins and their regulators: Roles in membrane transport, development and disease. Nat Rev Mol Cell Biol 12:362-375.

78. Zhao X, Lasell TKR, Melancİon P. 2002. Localization of Large ADP-Ribosylation Factor-Guanine Nucleotide Exchange Factors to Different Golgi Compartments: Evidence for Distinct Functions in Protein Traffic. Mol Biol Cell 13:119–133.

79. Ishizaki R, Shin H-W, Mitsuhashi H, Nakayama K. 2008. Redundant Roles of BIG2 and BIG1, Guanine-Nucleotide Exchange Factors for ADP-Ribosylation Factors in Membrane Traffic between the trans -Golgi Network and Endosomes. Mol Biol Cell 19:2650–2660.
80. Elbein AD. 1987. Inhibitors of the Biosynthesis and Processing of N-Linked Oligosaccharide Chains. Annu Rev Biochem 56:497–534.
81. Stirzaker SC, Whitfeld PL, Christie DL, Bellamy AR, Both GW. 1987. Processing of rotavirus glycoprotein VP7: implications for the retention of the protein in the endoplasmic reticulum. J Cell Biol 105:2897–903.
82. Petrie BL, Estes MK, Graham DY. 1983. Effects of tunicamycin on rotavirus morphogenesis and infectivity. J Virol 46:270–4.
83. Ruiz MC, Díaz Y, Peña F, Aristimuño OC, Chemello ME, Michelangeli F. 2005. Ca2+ permeability of the plasma membrane induced by rotavirus infection in cultured cells is inhibited by tunicamycin and brefeldin A. Virology 333:54–65.
84. Wessels E, Duijsings D, Niu T-K, Neumann S, Oorschot VM, de Lange F, Lanke KHW, Klumperman J, Henke A, Jackson CL, Melchers WJG, van Kuppeveld FJM. 2006. A Viral Protein that Blocks Arf1-Mediated COP-I Assembly by Inhibiting the Guanine Nucleotide Exchange Factor GBF1. Dev Cell 11:191–201.
85. Monetta P, Slavin I, Romero N, Alvarez C. 2007. Rab1b interacts with GBF1 and modulates both ARF1 dynamics and COPI association. Mol Biol Cell 18:2400–2410.
86. González RA, Torres-Vega MA, López S, Arias CF. 1998. In vivo interactions among rotavirus nonstructural proteins. Arch Virol 143:981–996.
87. Maruri-Avidal L, Lopez S, Arias CF. 2008. Endoplasmic Reticulum Chaperones Are Involved in the Morphogenesis of Rotavirus Infectious Particles. J Virol 82:5368–5380.
88. Gutierrez M, Isa P, Sanchez-San Martin C, Perez-Vargas J, Espinosa R, Arias CF, Lopez S. 2010. Different Rotavirus Strains Enter MA104 Cells through Different Endocytic Pathways: the Role of Clathrin-Mediated Endocytosis. J Virol 84:9161–9169.
89. Schindelin J, Arganda-Carreras I, Frise E, Kaynig V, Longair M, Pietzsch T, Preibisch S, Rueden C, Saalfeld S, Schmid B, Tinevez J-Y, White DJ, Hartenstein V, Eliceiri K, Tomancak P, Cardona A. 2012. Fiji: an open-source platform for biological-image analysis. Nat Methods 9:676–682.

FIGURE LEGENDS

871 **FIG. 1.** Inhibition of COPI/Arf1 activity reduces the production of viral progeny. MA104
872 cells were pre-treated for 30 min with BFA (A) or GCA (B) at the indicated concentrations.
873 Treated cells were infected with RRV at an MOI of 5 in the presence of the inhibitors for
874 1h, the unbound virus was removed, and fresh media containing the drugs was added. At 12
875 hpi the total virus obtained from cells and media were harvested, and the viral titer was
876 determined by an immunoperoxidase assay. The arithmetic means ± standard deviations
877 from three independent experiments performed in duplicate are shown. (C) MA104 cells
878 were infected with the indicated rotavirus strains (MOI of 5) in the presence of BFA
879 (0.5µg/ml), and the viral titer (ffu/ml) of the total virus was determined by an
880 immunoperoxidase assay. The arithmetic means ± standard deviations from two
881 independent experiments performed in duplicate are shown. (D) MA104 cells were
882 transfected with a siRNA to GBF1. Left panel, representative western blot analysis of cells
883 transfected with the indicated siRNA. The expression of GBF1 was detected with a specific
884 antibody. Vimentin (Vim) was used as a loading control. Right panel, at 72 hpt cells
885 transfected with either a scrambled or GBF1 siRNAs were infected with RRV (MOI=5). At
886 12 hpi, the total virus from cells and media was collected and the viral titer was determined.
887 Data represent the percentages of virus progeny, where the cells transfected with an
888 irrelevant siRNA (Irre), correspond to 100% infectivity. The arithmetic means ± standard
889 deviations from three independent experiments performed in duplicate are shown.
890 *=P<0.05, and **=P<0.01.

891 **FIG. 2.** BFA and GCA inhibit rotavirus replication at a post-entry step. (A) MA104 cells
892 were infected with RRV (MOI=5) at 37 °C for 1h. Unbound virus was removed, and 0.5
893 µg/ml of BFA or 10 µM of GCA were added at the indicated times post-infection. At 12hpi,

894 the total virus obtained from cells and media was recovered, and the viral titer was
895 determined. Cells Data represent the percentage of the virus progeny obtained from
896 untreated cells that correspond to 100% infectivity. The arithmetic means ± standard
897 deviations from two independent experiments performed in duplicate are shown.
898 *=P<0.05,. (B) Representative gel electrophoresis analysis of RRV particles produced at
899 different times post-infection. MA104 cells were infected with RRV (MOI=5) in the
900 absence of the inhibitors for 1 h at 37°C. Unbound virus was removed and fresh media was
901 added. At the indicated times post-infection the virus was semi-purified as described in
902 Materials and Methods (see "Enrichment of viral particles" section). The same proportion
903 of each sample was loaded onto the gel, which was silver stained. The migration pattern of
904 the viral structural proteins is indicated (right).

905 **FIG. 3.** BFA and GCA block the production of TLPs. (A) Isopycnic CsCl gradients of viral
906 particles assembled in the absence or presence of 0.5µg/ml BFA (A) or 10µM GCA (C).
907 (B) and (D) Gel electrophoresis analysis of the viral proteins in the bands detected in the
908 isopycnic gradients shown in panels A and C. The same proportion of each collected band
909 was loaded onto the gel, which was silver stained. The migration of the viral structural
910 proteins in the gels is indicated (right).

911 **FIG. 4.** BFA and GCA do not block the budding of rotavirus DLPs into the ER. MA104
912 cells untreated (A) or treated with 0.5µg/ml BFA (B) or 10µM GCA (C) were infected with
913 RRV at 250 viroplasm forming units per cell. At 6 hpi, the cells were fixed and processed
914 for transmission electron microscopy. The black arrowheads indicate the swollen vesicles
915 of the endoplasmtic reticulum observed in the presence of BFA or GCA. The open
916 arrowheads and asterisks denote TLPs and DLPs budding site in viroplams, respectively. V,

917 Viroplasm; Nu, nucleus; m, mitochondrion; AP, autophagosome; mt, microtubules; ER,
918 endoplasmatic reticulum; and GC, Golgi complex. Bar is 500 nm.

919 **FIG. 5.** Inhibition of the GBF1 activity changes the electrophoretic mobility of VP7 and
920 NSP4. (A) Autoradiography of mock infected or infected lysates (RRV, MOI of 5) in the
921 presence of BFA (0.5µg/ml) or GCA (10µM). At 7.5 hpi, the cells were pulse-labeled with
922 25 µCi/ml of ^{35}S-Met/Cys for 30 min and harvested at 10 hpi. (B) Fluorography of infected
923 lysates in the presence of BFA (0.5µg/ml) or GCA (10µM). At 6.5 hpi, the cells were
924 radiolabeled with 200 µCi/ml of ^{3}H-mannose for 1.5 h and harvested at 10 hpi. (C)
925 Autoradiography of lysates transfected with the indicated siRNA and mock-infected or
926 infected with RRV (MOI=5). At 7.5 hpi, the cells were pulse-labeled with 25 µCi/ml of ^{35}S-
927 Met/Cys. The migration pattern of the viral structural and non-structural proteins in the gels
928 is indicated (right).

929 **FIG. 6.** The alteration of the electrophoretic mobility of VP7 in the presence of BFA or
930 GCA is not related to modified glycosylation. (A) MA104 cells were pre-treated for 30 min
931 with BFA (0.5 µg/ml) or GCA (10 µM), and then, infected with wild type SA11 (SA11wt)
932 or the mutant SA11-CL28 strain, both at an MOI of 5, in the presence of inhibitors for 1 h.
933 Unbound virus was removed, and fresh media containing BFA or GCA was added. At 12
934 hpi, the cells were harvested, and the viral titer was determined. Data represent the virus
935 progeny relative to untreated cells. The arithmetic means ± standard deviations from two
936 independent experiments performed in duplicate are shown. *=P<0.05. (B) Representative
937 western blot analysis of proteins from untreated (control), BFA- or GCA-treated cells
938 infected with SA11wt or SA11-CL28 at 8hpi. Expression of structural viral proteins were
939 detected with an anti-rotavirus polyclonal serum raised against purified TLPs. Vimentin

(Vim) was used as a loading control. The migration pattern of the viral structural proteins in the gels is indicated (right). The asterisks mark the position of the slow-migrating VP7 protein.

Fig. 7. BFA- and GCA-induced modification of VP7 electrophoretic mobility is related neither to N-/O-glycosylation nor to phosphorylation. MA104 cells were transfected with a plasmid coding for the VP7 protein of RRV and treated with BFA or GCA (5 µg/ml) at 1 hpt. At 18 hpt the cells were lysed, and the lysate underwent treatment with either of the following enzymes: (A) PNGaseF (Peptide-N-Glycosidase F), which removes almost all types of N-linked (Asn-linked) glycosylation or EndoH (endo-β-N-acetylglucosaminidase-H), which removes only high mannose and some hybrid types of N-linked carbohydrates; (B) a protein deglycosylation mix, which in addition to all N-linked glycans removes many common O-linked glycans; (C) λ-phospatase, a protein phosphatase with activity towards phosphorylated serine, threonine and tyrosine residues. The figure shows a representative western blot of the cell extracts incubated with the enzymes indicated. Expression of the VP7 protein was detected with a specific antibody. The glycosylated (gVP7) and deglycosylated (VP7) forms of VP7 are indicated. Tubulin (TUB) was used as loading control. (D) Representative western blot of MA104 cells expressing a recombinant RRV VP7 protein with the N-glycosylation site mutated (69-NST-71 to 69-QSG-71); BFA (2.5 µg/ml) was added at 1 hpt and the cells were lysed at 18 hpt. The expression of non-glycosylated VP7 was detected with a specific antibody.

FIG. 8. BFA and GCA inhibit the trimerization of the glycosylated and non-glycosylated forms of VP7. Immunofluorescence of MA104 cells infected with RRV (A), SA11wt (B), or SA11-CL28 (C) at an MOI of 1 in the absence or presence of BFA (0.5 µg/ml) or GCA

(10 µM). At 6 hpi, the cells were fixed and co-immunostained with either antibodies against NSP2 (red) and VP7 trimers (MAb159, green) (upper row) or NSP2 (red) and VP7 monomers (M60, green) (lower row). The nuclei (blue) were stained with DAPI. The open box corresponds to amplified images at the right column of each image. Scale bar is 10 µm.

FIG. 9. Silencing the expression of GBF1 blocks VP7 trimerization. Immunofluorescence of MA104 cells transfected with the indicated siRNA and at 72 hpt, cells were infected with RRV (MOI, 3). At 6 hpi, the cells were fixed and co-immunostained with antibodies against either NSP2 (red) and VP7 trimers (Mab159, green) (upper panel) or NSP2 (red) and VP7 monomers (M60, green) (lower panel). The cells nuclei (blue) were stained with DAPI. The open box corresponds to magnified images shown at right. Scale bar is 10 µm.

FIG. 10. Silencing the expression of NSP4 inhibits the trimerization of VP7. Immunofluorescence of MA104 cells stably expressin NSP5-EFGP (magenta), which were transfected with the indicated siRNA, and infected with RRV (MOI, 3) at 72 h post-transfection. At 6 hpi, cells were fixed and co-immunostained with antibodies against either NSP4 (red) and VP7 trimers (MAb159, green) (upper row) or NSP4 (red) and VP7 monomers (M60, green) (lower row). Cells nuclei (blue) were stained with DAPI.. Scale bar is 10 µm.

FIG. 11. NSP4 facilitates the VP7 trimerization. Immunofluorescence of Hek293-T7 RNA polymerase cells co-transfected with the VV capping enzyme expression plasmids (D1R and D12L) and either a plasmid encoding for non-glycosylated VP7, NSP4, or a combination of both plasmids. At 24 hpt, the cells were fixed and co-immunostained with antibodies directed either to NSP4 (red) and VP7 monomers (M60, green) or NSP4 (red)

and VP7 trimers (MAb159, green). The cells nuclei (blue) were stained with DAPI. Scale bar is 10 µm.

Fig 12. GBF1 catalytic activity but not Arf1 activation is essential for rotavirus replication. (A) Schematic map of GBF1 domain organization and of truncated mutants used in this study, in which the amino acid substitutions are indicated. Numbers in parenthesis indicate GBF1 amino acids. (B) Hek293 cells were transfected with the different GBF1 mutant plasmids, and at 24 hpt cells were pre-treated for 30 min with BFA (0.5 µg/ml), and then, infected with RRV at an MOI of 5, in the presence of BFA for 1 h. Unbound virus was removed, and fresh media containing BFA was added. At 12 hpi, the cells were harvested, and the viral titer was determined. Data represent the virus progeny relative to untreated cells. The arithmetic means ± standard deviations from three independent experiments performed in duplicate are shown. *=P<0.05. (C) MA104 cells were transfected with a siRNA to Arf1. Left panel, representative western blot analysis of cells transfected with the indicated siRNA. The expression of Arf1 was detected with a specific antibody. Vimentin (Vim) was used as a loading control. Right panel, at 72 hpt scramble siRNA and siArf1cells were infected with RRV (MOI=5). At 12 hpi, cells were collected and the viral titer was determined. Data represent the percentages of virus progeny, where the cells transfected with an irrelevant siRNA (Irre), correspond to 100% infectivity. The arithmetic means ± standard deviations from three independent experiments performed in duplicate are shown.

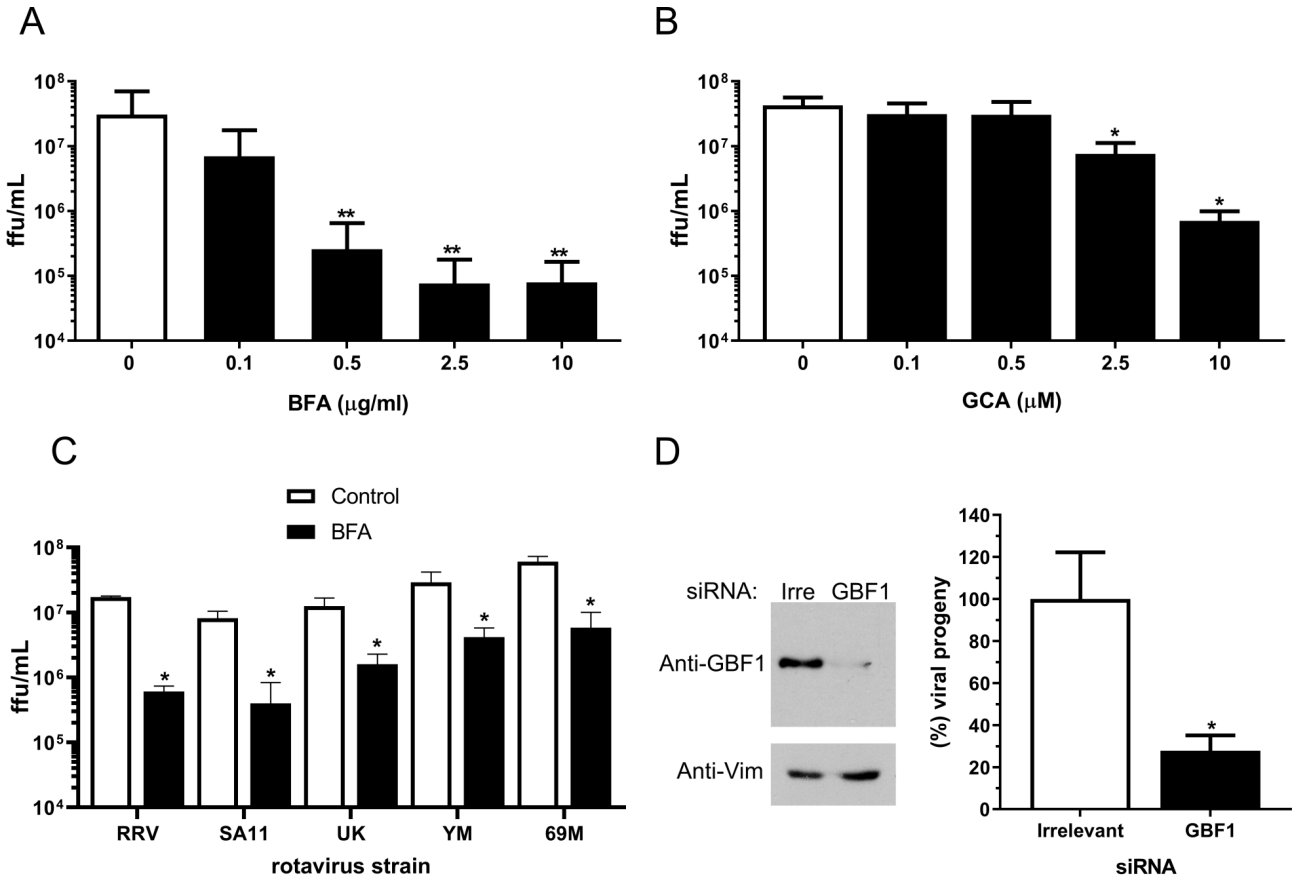

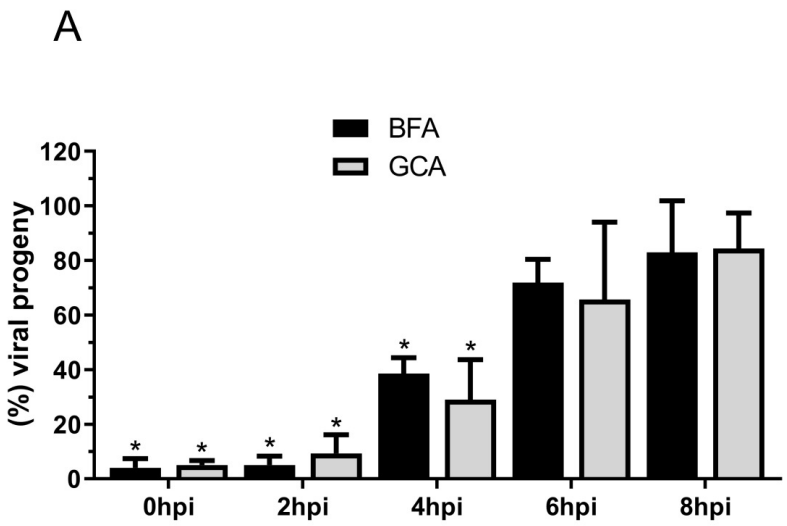

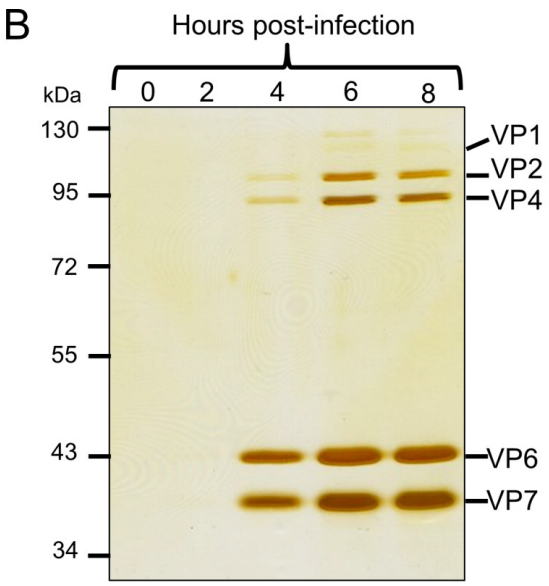

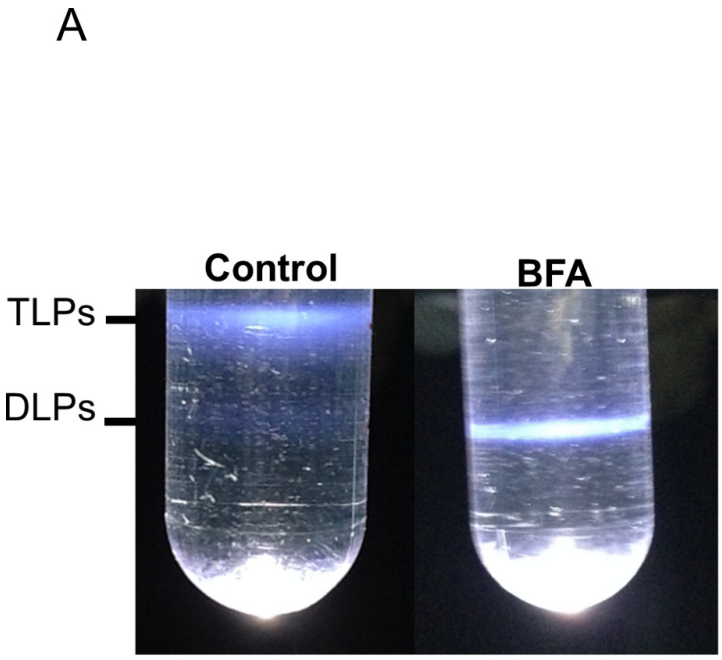

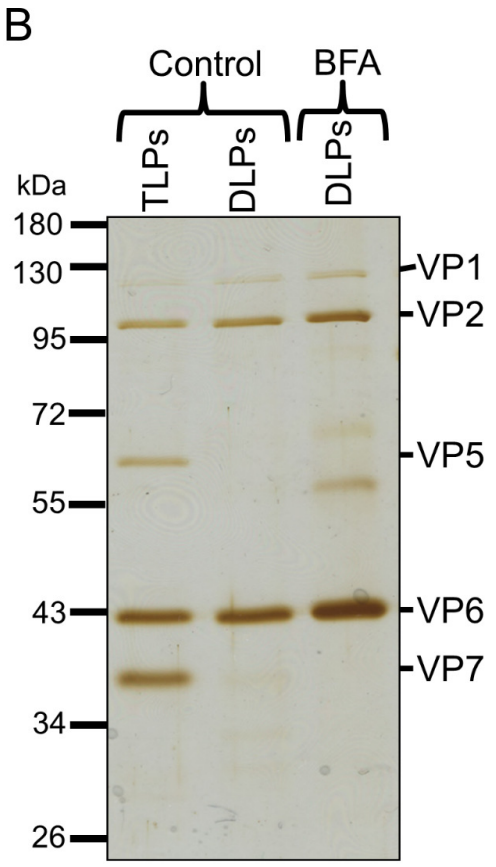

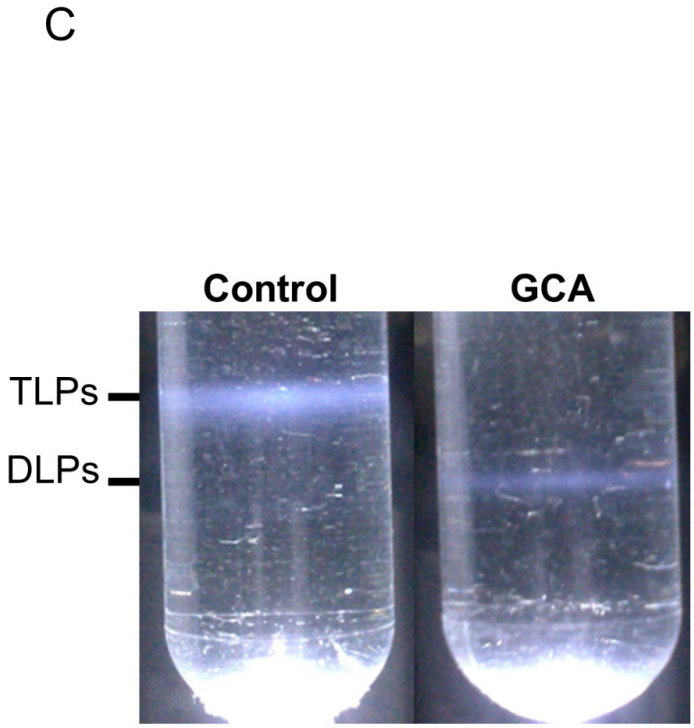

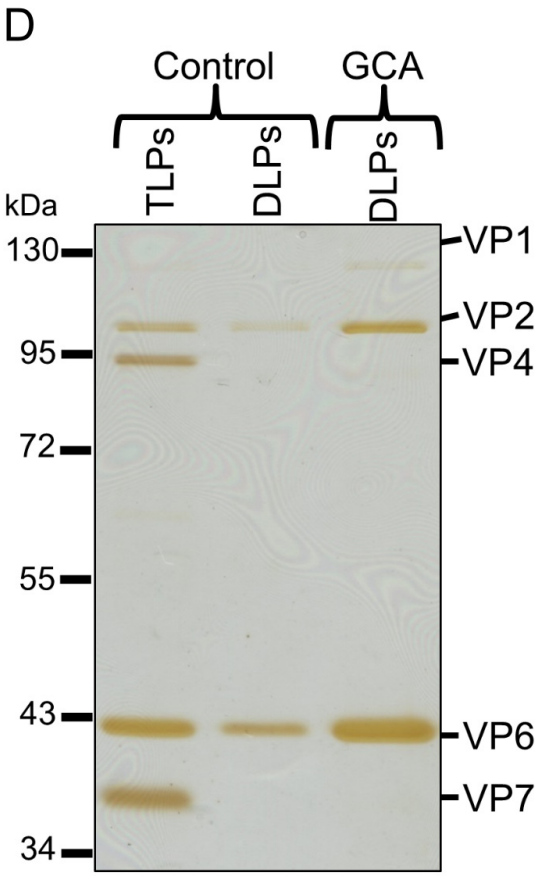

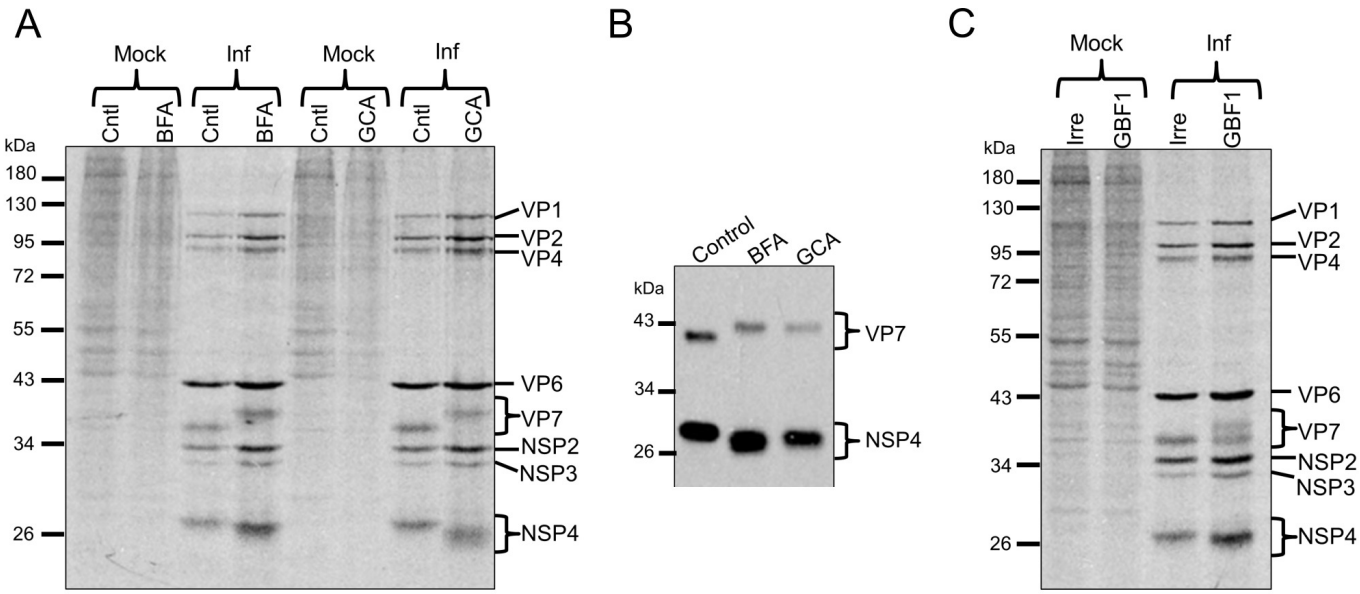

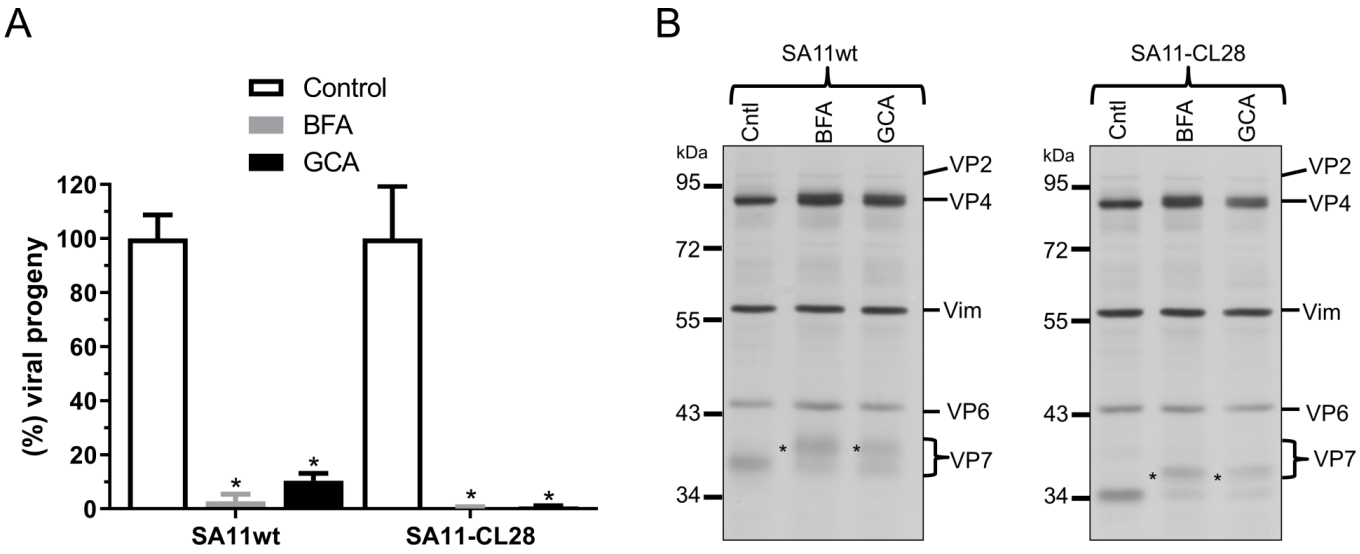

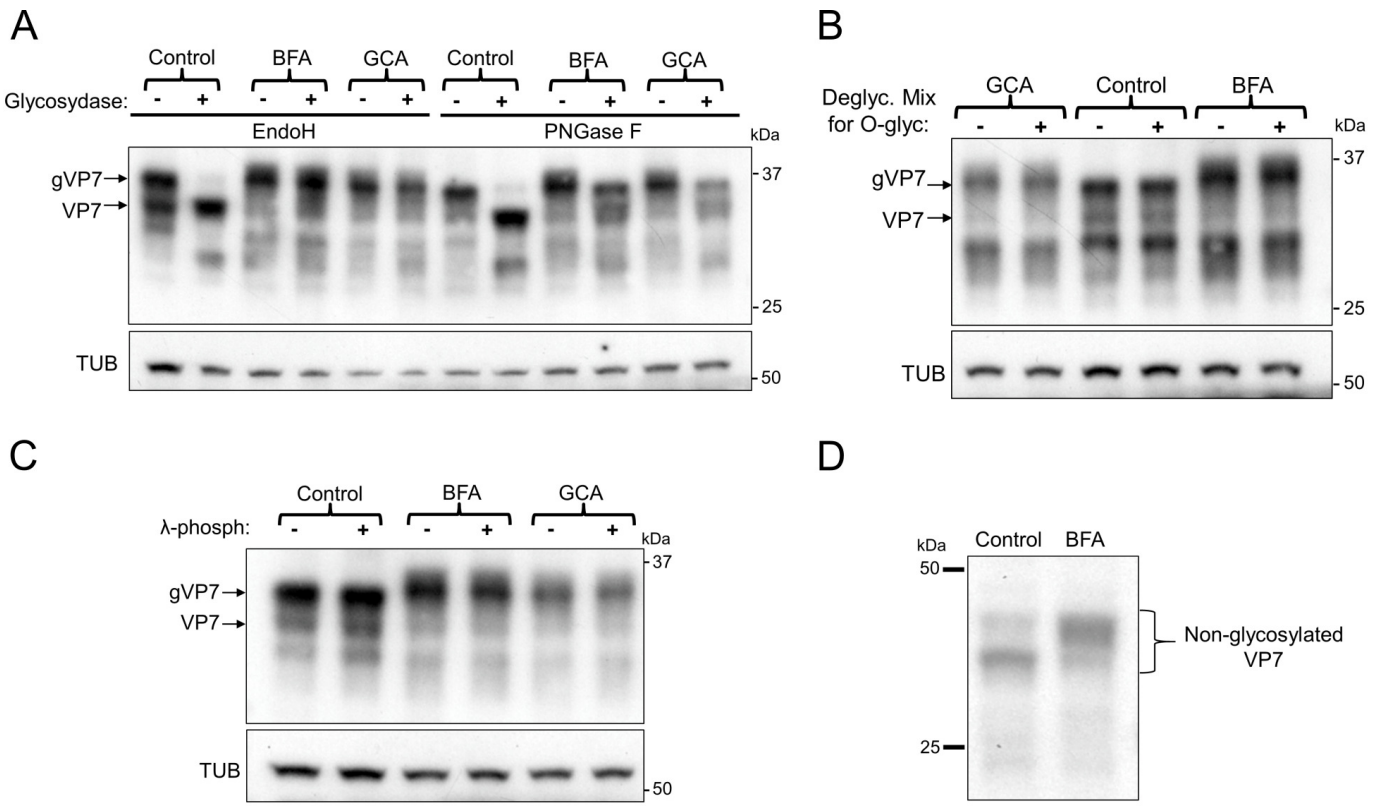

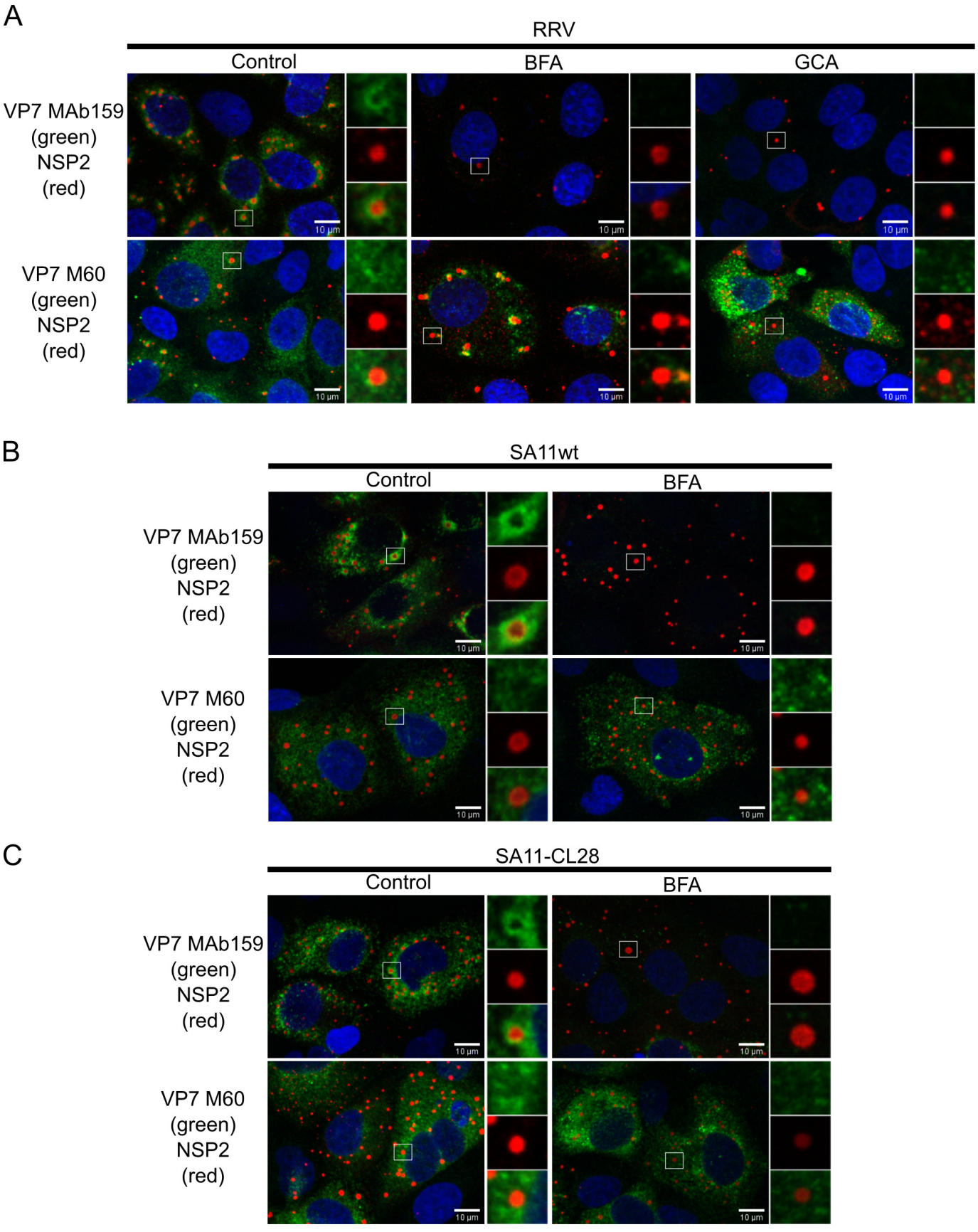

Journal of Virology
JVI
Journal of Virology